Master's Thesis

Validation of HT-29 cell differentiation protocol and the use of HT-29 cell model as an infection model

Jenni Auramo

University of Jyväskylä

Department of Biological and Environmental Science

31 May 2023

UNIVERSITY OF JYVÄSKYLÄ, Faculty of Mathematics and Science
Department of Biological and Environmental Science
Degree program: Master's Degree Program in Cell and Molecular Biology

Auramo, Jenni	Validation of HT-29 cell differentiation protocol and the use of HT-29 cell model as an infection model
MSc Thesis	47 p., 0 appendices
Supervisors:	Professor Lotta-Riina Sundberg and post-doctoral researcher Kati Karvonen
Revisors:	Professor Janne Ihalainen and PhD Riitta Nissinen
Month Year	May 2023

Keywords: cell model, host-pathogen interaction, *in vitro*, mucus

Knowledge of host-pathogen interaction is important for understanding different microbes and their behaviour. *In vitro* cell models are important tools in research to examine host-pathogen interaction and the behaviour of pathogens and they are especially needed with bacterial research, because mammalian cell models resemble the *in vivo* conditions better than traditional bacterial culture. There are several viruses and bacteria, for example enteroviruses and *Pseudomonas aeruginosa* bacterium, that cause infections towards which there is no cure, or the infections are difficult to treat. Especially studies of the properties of *Pseudomonas aeruginosa* bacterium in *in vitro* cell models are needed because the bacterium is resistant to various antibiotics and causes hospital-acquired infections. The aim of this study was to establish and validate a novel HT-29 cell model and its differentiation protocol for research use at the University of Jyväskylä. The hypothesis was that this cell line can be differentiated into mucus producing cells which can be of versatile use in the future. The cells were cultured in a specific topographic surface for eight days to differentiate them into mucus-producing cells. The differentiated cells were stained with Alcian blue stain and tested with MUC2, villin, and lysozyme antibodies to verify their differentiation and mucus production. Additionally, the differentiated and undifferentiated HT-29 cells were infected with coxsackievirus A9, coxsackievirus B3, coronavirus OC43, *Pseudomonas aeruginosa* strains PA14 and 573, *Salmonella enterica* serovar *typhimurium, Streptococcus mutans* and *Acinetobacter baumannii* to discover which of the microbes infect the cells and thus, could be utilised for research in the future. The antibody test results did not fully confirm successful differentiation of the cells, but Alcian blue staining did. From the tested pathogens, enteroviruses and both *Pseudomonas aeruginosa* strains infected the cells and can be used as an infection model in the future with these cells. *Salmonella enterica* serovar *typhimurium* infected both cells mildly, while *Streptococcus mutans* infected mildly only the undifferentiated cells. *Acinetobacter baumannii* was not infective. The use of differentiated mucus producing cells expands the future research possibilities. Studying the functions of the mucus against pathogens and infections gives valuable information about the immune response of the mucous membranes and can help in understanding the different phases of infections and in developing new medical approaches against pathogens.

JYVÄSKYLÄN YLIOPISTO, Matemaattis-luonnontieteellinen tiedekunta
Bio- ja ympäristötieteiden laitos
Tutkinto-ohjelma: Solu- ja molekyylibiologian maisteriohjelma

Auramo, Jenni	HT-29 solujen erilaistamisprotokollan ja solumallin infektiomallina käytön validointi
Pro gradu tutkielma:	47 s., 0 liitettä
Työn ohjaajat:	Professori Lotta-Riina Sundberg ja tutkijatohtori Kati Karvonen
Tarkastajat:	Professori Janne Ihalainen ja FT Riitta Nissinen
Kuukausi Vuosi	Toukokuu 2023

Hakusanat: in vitro, isäntä-patogeeni-vuorovaikutus, lima, solumalli

In vitro -solumallit ovat tärkeitä työkaluja isäntä-patogeeni-vuorovaikutuksen ja mikrobien käyttäytymisen tutkimuksessa, ja niitä tarvitaan erityisesti bakteeritutkimuksessa, sillä nisäkässolumallit vastaavat paremmin *in vivo* -ympäristöä kuin pelkkä bakteeriviljely. Lukuisat virukset ja bakteerit, kuten enterovirukset ja *Pseudomonas aeruginosa* -bakteeri, aiheuttavat infektioita, joita vastaan ei ole parannuskeinoa, tai infektioiden hoitaminen on vaikeaa. Etenkin *Pseudomonas aeruginosa* -bakteerin tutkiminen *in vitro* -solumalleissa on tärkeää, sillä bakteeri on vastustuskykyinen useille antibiooteille ja aiheuttaa sairaalaperäisiä infektioita. Tämän tutkimuksen tavoitteena oli perustaa ja validoida uusi HT-29 solumalli ja sen erilaistamisprotokolla tutkimuskäyttöön Jyväskylän yliopistolle. Hypoteesina oli, että tämä solumalli voidaan erilaistaa limaa tuottaviksi soluiksi, joita voidaan monipuolisesti käyttää jatkossa infektiomallina. Solut erilaistettiin limaa tuottaviksi soluiksi kasvattamalla niitä kahdeksan päivää topografisella pinnalla. Erilaistuneet solut värjättiin Alcian blue -värillä ja testattiin MUC2, villiini ja lysotsyymi vasta-aineilla erilaistumisen ja liman tuoton toteamiseksi. Lisäksi erilaistuneet ja erilaistumattomat HT-29 solut infektoitiin coxsackie A9 enteroviruksella, coxsackie B3 enteroviruksella, OC43 koronaviruksella, *Pseudomonas aeruginosa* -bakteerin kannoilla PA14 ja 573, *Salmonella enterica* -bakteerin *typhimurium* -serotyypillä, *Streptococcus mutans* -bakteerilla ja *Acinetobacter baumannii* -bakteerilla, jotta nähdään mitkä patogeeneistä kykenevät infektoimaan näitä soluja ja minkä patogeenien tutkimiseen tätä solulinjaa voidaan tulevaisuudessa käyttää. Vasta-ainetestit eivät kunnolla osoittaneet erilaistumisen onnistumista, mutta Alcian blue -värjäys osoitti. Testatuista patogeeneistä enterovirukset ja molemmat *Pseudomonas aeruginosa* -kannat infektoivat soluja ja niitä voi tutkia HT-29 solumallissa jatkossakin. *Salmonella enterica* bakteerin *typhimurium* -serotyyppi infektoi lievästi molempia soluja ja *Streptococcus mutans* lievästi vain erilaistumattomia soluja. *Acinetobacter baumannii* ei ollut infektiokykyinen. Erilaistettujen limaa tuottavien solujen käyttö laajentaa tutkimusmahdollisuuksia. Tutkimus liman ominaisuuksista patogeenejä ja infektioita vastaan antaa arvokasta tietoa limakalvojen immuunivasteesta ja auttaa ymmärtämään infektion eri vaiheita ja kehittämään uusia lääkkeitä patogeenejä vastaan.

TABLE OF CONTENTS

TERMS AND ABBREVIATIONS

HT-29	Human colorectal adenocarcinoma cell line
CVA9	coxsackievirus A9
CVB3	coxsackievirus B3
MUC2	Mucin 2 Oligomeric Mucus/Gel-Forming
DAPI	4′,6-diamidino-2-phenylindole
RT	Room Temperature
Pfu	Plaque-forming unit
MOI	Multiplicity of Infection
CPE	Cytopathic Effect
DIF	Differentiated HT-29 cells
unDIF	unDifferentiated HT-29 cells
RA 546	anti-rabbit 546 antibody

1 INTRODUCTION

Understanding the host-pathogen interaction is important when studying infectious diseases and their cure and prevention (Schmidt and Völker 2011). Information about the pathogen´s abilities to invade host cells and tissues and to colonise and infect them can be obtained by studying the different phases of the infection, gaining information that helps in developing novel drugs and vaccines (Southwood and Ranganathan 2019). Host-pathogen interaction causes molecular and metabolic changes in both the pathogen and the host (Hsu and Du Pasquier 2015).

The pathogens must have specific abilities for invading the host cell and for surviving the possible defence mechanisms of the host cell (Ashida et al. 2011). Additionally, the pathogen has to be able to adjust its behaviour, functions, and gene expression so that it can survive the host cell's variable conditions concerning metabolism, pH, and oxygen levels, for example (Unden et al. 2016). Furthermore, the pathogen can colonise the host, infect it, or it can be opportunistic (Madigan et al. 2015). A colonising pathogen invades the host and resides in the host, but remains asymptomatic (Le Guennec et al. 2020). An opportunistic pathogen resides asymptomatic in the host, but it can become pathogenic if there is for example a decrease in host immune defence or the pathogen invades a new tissue through a wound (Brown et al. 2012).

Bacteria are usually studied in bacterial culture, but growing the bacteria in cell lines better illustrates the actions of the bacteria with the host (Kim et al. 2010). *In vitro* cell models that represent and mimic the real *in vivo* surroundings of host-pathogen interaction as precisely as possible are important for research of pathogens, their functions, and their infection mechanisms (Crabbé et al. 2014). As viruses need a host to replicate, they have been studied in various *in vitro* human cell models for decades (Leland and Ginocchio 2007). These cell models can also be utilised in bacterial studies. At least lung carcinoma epithelial A549 cells, cervical epithelial HeLa cells, ileocecal epithelial Caco-2 cells, and cystic fibrosis IB3 and C38 epithelial cell lines have been used as cell models in bacterial infection studies along with the HT-29 cells investigated in this study (Eckmann et al. 1993, Kim et al. 1998, Sears 2000, Laparra and Sanz 2009, Kim et al. 2010, Yu et al. 2011, Kortman et al. 2012, Parker et al. 2012, Antunes et al. 2013, Barron et al. 2021).

1.1 HT-29 colorectal adenocarcinoma cells

The HT-29 cells are a human colorectal adenocarcinoma cell line (Simon-Assmann et al. 2007). They have been used earlier to study human colorectal cancer biology, but nowadays the interest is more in their similarities in

properties and protein expression with human small intestine cells (Martínez-Maqueda et al. 2015). In general, there are three types of human intestinal epithelial cells; enterocytes, Paneth cells, and mucus producing goblet cells (Birchenough et al. 2015). The goblet cells secrete glycoproteins known as gel-forming mucins, majority of which is MUC2 mucin, that create the mucus layer that covers the gastrointestinal tract (Dong et al. 2012, Pelaseyed et al. 2014).

The intestinal mucus has many functions concerning both the gut microbiome of the intestines and pathogenic invading pathogens (Knoop and Newberry 2018). The mucus layer protects the epithelial cells from microbes as a physical barrier and provides nutrients to the gut microbiome (Gagnon et al. 2013). The goblet cells secrete mucus proteins and IgA antibodies to the mucus layer, while the Paneth cells secrete lysozymes, antimicrobial peptides, and phospholipases to the mucus layer and together these antibacterial mediators aim to neutralise the invading pathogens (Pelaseyed et al. 2014, Herath et al. 2020). However, despite the defence mechanisms of the intestinal mucus, some pathogens are still able to invade the mucus layer and cause infection (Birchenough et al. 2015).

Studying the functions of the intestinal mucus and its antimicrobial defence mechanisms gives valuable information about the role of the mucus in pathology of diseases and cancers (Dong et al. 2012). The HT-29 cell line is a beneficial cell model for studying the role of the mucus as the HT-29 cells can be differentiated to different cell types depending on the growth surroundings (Park et al. 2018). For example, in the presence of glucose the cells remain unchanged, but in a glucose-free medium or when exposed to colchicine, the cells start to differentiate containing both enterocyte-like cells and mucus producing goblet cells (Centonze et al. 2022).

1.2 Enteroviruses

Enteroviruses are a large group of viruses belonging to the picornavirus family infecting pigs, bovine animals, primates, and humans (Chen et al. 2020). Enteroviruses are icosahedral, enveloped, small (diameter 28-30 nm) single-stranded RNA-viruses (Wang et al. 2020). They are divided to rhinovirus species A to C and enterovirus species A to L, from which species A to D infect humans, all including several different enterovirus types like coxsackie A9 (CVA9) and coxsackie B3 (CVB3) from species group B (Chen et al. 2020). Enteroviruses usually transmit through faecal-oral route (Zhu et al. 2021). The viral replication and primary infection occur in the mucous membranes of the intestines (Muehlenbachs et al. 2015). Enterovirus infections can be symptomless, but the viruses also cause a variety of acute, chronic, and long-term infections (Muir 2017). In addition to intestinal infections, enteroviruses cause myocarditis, skin symptoms, respiratory tract infections, and encephalitis (Nikonov et al. 2017).

CVA9 is an enterovirus that despite its name A9 belongs to the B species of enteroviruses, because it is genetically closer to B species viruses, though it is

pathogenically more like A species viruses (Hietanen and Susi 2020). It is an important human pathogen and one of the most pathogenic and prevalent enteroviruses (Heikkilä et al. 2016). CVA9 causes a variety of diseases like persistent diarrhoea, myocarditis, aseptic meningitis, acute flaccid paralysis, respiratory illnesses, and hand, foot, and mouth disease (Zhao et al. 2022). CVA9 transmits through airborne droplets, faecal-oral route and in direct contact, and both asymptomatic and symptomatic infected persons can spread the virus to others (Zhao et al. 2022). The virus capsid of CVA9 contains the typical enterovirus capsid proteins VP1-VP4, but the capsid protein VP1 has an Arg-Gly-Asp (RGD) peptide motif in its C-terminal, which is a specific feature of CVA9 (Huttunen et al. 2014). The virus uses this motif to interact with receptors on the cell surface (Heikkilä et al. 2009).

CVB3 belongs to the B species, and it is also a highly prevalent and pathogenic human pathogen (Pinkert et al. 2011). The main tissues CVB3 targets are pancreas and heart, but also lung, intestine, liver, testis, prostate, and brain can be infected (Massilamany et al. 2014). CVB3 usually causes a mild illness with flu-like symptoms, but it can also cause acute or chronic pancreatitis, myocarditis, and meningitis (Geisler et al. 2021). The chronic myocarditis caused by CVB3 can lead to dilated cardiomyopathy and heart failure with prolonged viral persistence (Pinkert et al. 2011).

1.3 Human coronavirus hCoV-OC43

Coronaviruses are the largest virus group belonging to the *Coronaviridae* family that is further divided to α, β, γ, and δ groups (Szczepanski et al. 2019). They infect birds and mammals like humans, dogs, cats, horses, cattle, bats, swine, mice and many more (Zhang et al. 2018). Coronaviruses are single positive-stranded RNA viruses with an envelope and a crown-like appearance due to the club-shaped spike proteins on their surface, from which their name is derived (Zhao et al. 2020). These viruses usually transmit through droplets and aerosols or when touching surfaces contaminated with them (Singhal 2020).

Usually coronaviruses cause a mild flu-like respiratory illness, but they can also cause gastroenteritis, more severe lower respiratory tract infections, and sometimes life-threatening pneumonia and bronchiolitis in the elderly, children, infants, and immunocompromised individuals (Liu et al. 2021). Human coronavirus hCoV-OC43 (OC43) belongs to the β subgroup of coronaviruses, and it is the most prevalent coronavirus in humans (Jean et al. 2013, Zhang et al. 2018). It causes usually mild upper respiratory tract infections occurring mostly in winter and early spring, but it can also cause lethal encephalitis in immunocompromised individuals (Szczepanski et al. 2019, Schirtzinger et al. 2022). OC43 replicates in the respiratory epithelium cells (Schirtzinger et al. 2022).

1.4 Pseudomonas aeruginosa

Pseudomonas aeruginosa is a rod-shaped, Gram-negative gammaproteobacterium with ability to infect humans, animals, and plants (Botelho et al. 2019). In humans, the bacterium is involved in both acute and chronic infections as an opportunistic bacterium (Madigan et al. 2015). *P. aeruginosa* has an ability to create biofilms, making it more resistant to antibiotics and enhancing the formation of chronic infection (Ciofu and Tolker-Nielsen 2019). A biofilm is a mucous matrix usually attached to a surface, consisting of aggregated bacteria covered with polysaccharides, extracellular DNA, and proteins (Vestby et al. 2020). It has genetic, physical, and physiological ways of resistance towards antibiotics and environmental stresses, which prevent the antibiotics and environment from affecting the bacteria inside the biofilm (Lopez et al. 2010).

In addition to biofilm formation, *P. aeruginosa* has many other features that make it pathogenic and difficult to treat (Mulcahy et al. 2014). It survives under both aerobic and anoxic conditions due to its versatile energy metabolism containing oxidases and denitrification enzymes (Ramos et al. 2015). *P. aeruginosa* has pili and flagella that help its motility and adherence to surfaces (Cepas and Soto 2020). The bacterium produces a variety of virulence factors like pyocyanin, protease, and alkaline phosphatase which suppress the host immune response and toxins like exotoxin A, exoS, exoU, and exoT that inhibit the host inflammasome (Ramos et al. 2015).

Additionally, *P. aeruginosa* has a combination of adaptive (expression of efflux pumps, biofilm formation), intrinsic (low outer membrane permeability), and acquired (spontaneous mutation, horizontal gene transfer) resistance towards antibiotics (Botelho et al. 2019). *P. aeruginosa* is one of the six so called "ESKAPE"-group (*Enterococcus faecium, Staphylococcus aureus, Klebsiella pneumoniae, Acinetobacter baumannii, P. aeruginosa* and *Enterobacter* species) bacteria that have a great role in nosocomial infections and a special ability to evade the antimicrobial properties of antibiotics (Ciofu and Tolker-Nielsen 2019). *P. aeruginosa* is also on the World Health Organisation´s (WHO) list of important pathogens that should be studied more, and novel antibiotics should be developed against these pathogens (Botelho et al. 2019).

PA14 is a high-virulence strain of *P. aeruginosa* which has two pathogenicity factors (PAPI-1 and PAPI-2) in its genome that increase the virulence of the bacterium and its ability to infect multiple hosts (He et al. 2004). Mikkelsen and colleagues (2011) have also studied that the hypervirulent PA14 strain has adopted a mutation in ladS-gene which affects its functioning. The mutation lessens biofilm formation, but increases the type III secretion system (T3SS), expression of which increases the cytotoxicity of the strain towards mammalian cells and is involved in acute infections (Mikkelsen et al. 2011). The increase of cytotoxicity makes the strain more virulent (Mikkelsen et al. 2011)

1.5 Salmonella enterica serovar typhimurium

Salmonella genus consists of facultative anaerobic, rod-shaped, Gram-negative bacteria belonging to the *Enterobacteriaceae* family (Andino and Hanning 2015). The genus is further divided into two species, *S. bongori* and *S. enterica*, from which the latter is subdivided into six subspecies called *enterica* (I), *salamae* (II), *arizonae* (IIIa), *diarizonae* (IIIb), *houtenae* (IV) and *indica* (VI) (Eng et al. 2015). *Typhimurium* is a serovar of *enterica* subspecies that is able to infect both humans and animals like rodents, swine, poultry, and cattle (Spector and Kenyon 2012). In humans, *S. typhimurium* infection usually causes acute and chronic gastroenteritis, but meningitis and bacteraemia can also occur (Wattiau et al. 2011, Kröger et al. 2012).

S. typhimurium is transmitted through faecal-oral route via contaminated water or food by adhering to and penetrating the small intestines' intestinal epithelium (Gal-Mor et al. 2014). The invasion of the epithelium is possible by a characteristic ability of *S. typhimurium* to induce its own phagocytosis inside the cell (Eng et al. 2015). The virulence genes that enable this characteristic behaviour are clustered in two *Salmonella* pathogenicity islands called SPI-1 and SPI-2 which encode type III secretion systems (T3SSs) (Moreira et al. 2010). SPI-1 encoded T3SS is involved in cell invasion and SPI-2 encoded T3SS is involved in evading the host cell immune response, ability to survive in macrophages, and replication of the bacteria (Lamas et al. 2018).

1.6 Streptococcus mutans

Streptococcus mutans is a facultative anaerobic, Gram-positive cocci-shaped bacterium belonging to *Streptococcus* genus (Merritt and Qi 2012). Primarily the bacterium resides in mouth, pharynx, and intestines (Forssten et al. 2010). It infects the oral cavity and is the main pathogen causing dental caries, but it can also cause a life-threatening subacute bacterial endocarditis (Lemos et al. 2019). *Str. mutans* forms a mixed biofilm, commonly known as dental plaque, on the tooth surface with other primary colonisers and secondary organisms (Metwalli et al. 2013). It has evolved a set of glycosyltransferase enzymes that convert sucrose into extracellular polymer glucan which helps the bacterium to attach tightly to the dental surface and form biofilm (Lemos et al. 2019). *Str. mutans* also produces acids from glycolytic end-products, thus promoting acidic environment where it survives better than other organisms (Baker et al. 2017). One major virulence factor that *Str. mutans* has is the production of bacteriocins known as mutacins, which protect the bacterium against other pathogens in the oral cavity (Matsumoto-Nakano 2018).

1.7 Acinetobacter baumannii

Acinetobacter baumannii is an aerobic, Gram-negative, opportunistic coccobacillus belonging to the genospecies 2 of *Acinetobacter* genus (Chuang et al. 2011). It is the most common clinical *Acinetobacter* species worldwide (Cerqueira and Peleg 2011). Due to its ability to contaminate environmental surfaces and healthcare instruments, it is one of the main pathogens that causes infections in hospitals and healthcare units, especially among immunocompromised patients and in intensive care units, where these nosocomial infections lengthen the hospital stay and have a higher mortality rate (Chuang et al. 2011). In hospitals, *A. baumannii* causes secondary meningitis, infections in urinary tract, wounds, soft tissues, blood stream, and skin, and ventilator-associated pneumonia with high mortality rate (Cerqueira and Peleg 2011). It can also infect outside the hospital surroundings causing bacteraemia, pneumonia, endocarditis, secondary meningitis, and soft tissue, skin, and ocular infections, but these are less common (Antunes et al. 2014).

A. baumannii has many factors that aid its survival, persistence, and ability to infect (Howard et al. 2012). It can form biofilms which protect the bacteria on dry surfaces of hospital environment and medical devices (Morris et al. 2019). Also, it effectively adheres to human epithelial cells and invades and colonises them, targeting especially moist tissues like mucous membranes and wounds (Cerqueira and Peleg 2011, Howard et al. 2012). Most importantly *A. baumannii* has developed resistance against various antibiotics which is why it, just like *P. aeruginosa*, is one of the "ESKAPE"-group bacteria identified by WHO (Howard et al. 2012).

1.8 Aims of the study

Enteroviruses and *P. aeruginosa* both cause various infections that are untreatable, or difficult to cure. Studying these microbes gives valuable information about their behaviour and life cycle and can create possibilities for developing novel treatments against them. It is also important and interesting to know, what is the role of the mucus produced by the cells against pathogens, and whether the mucus provides protection for the cells. To study these features, a novel *in vitro* cell model is needed for the University of Jyväskylä (JYU). The HT-29 cells studied in this thesis have been used as an *in vitro* cell model in *P. aeruginosa* studies (Olson et al. 1999, Gagnon et al. 2013) and it seems to be a good cell model for bacterial studies.

The aims of this study were to establish the new HT-29 *in vitro* cell model for JYU and validate the differentiating protocol of the cells. The differentiated mucus-producing cells could give valuable information about the role of the mucus against pathogens. The hypothesis of this study was that the cells will differentiate to mucus-producing cells and the HT-29 cell line can be diversely used in future studies as an infection model. There were two specific study

questions: is the cell differentiation clearly detected and can it be demonstrated? Which of the tested pathogens can infect these cells and thus be studied with this cell line? To study these questions, the differentiated (DIF) and undifferentiated (unDIF) HT-29 cells were stained with specific mucus-dying stain, tested with differentiation-associated antibodies, and the pathogen infectivity was examined by determining cell viability after infection with various viruses and bacteria.

2 MATERIALS AND METHODS

2.1 Cell culture

The HT-29 colorectal adenocarcinoma cells (HTB-38, ATCC) were grown in McCoy's 5A 1X medium (Gibco) supplemented with 10% FBS (Gibco), 1% GlutaMax (Gibco), and 1% Penicillin/Streptomycin (Gibco) in conical 75 cm^2 cell culture flasks. The cells were sub-cultured every 2-3 days by detaching them from the cell bottle with 0.05% Trypsin-EDTA in PBS, counting them, and resuspending the cells to a density of 1.5 x 10^6 in total volume of 15 ml.

2.2 Cell differentiation

The HT-29 cells were differentiated to mucus producing DIF cells in a 1 cm x 1 cm generation G0 template topographic silica surface (Encytos B.V, Netherlands) following the protocol of Centonze and colleagues (2022). The surface was placed in a 12-well plate and sterilised with UV-light for 1 h. The unDIF HT-29 cells were cultured on the topographic surface in a density of 20 000 cells. 50 µl of cell suspension was added evenly on the surface and incubated for 4 h at +37 °C. After the incubation, the piece was covered with 1 ml of fresh cell medium (McCoy´s 5A 1X medium, described in detail in Section 2.1) and incubated for 8 d at +37 °C. The cell medium was changed to fresh medium every 3 days.

On the 8th day, the cells were collected from the topographic surface by aspirating away the cell medium, washing the cells twice with 0.5 ml of PBS, detaching the cells with 0.7 ml of Trypsin-EDTA in PBS for 4 min, adding 2.1 ml of cell culture media, centrifuging the cell suspension at 740 x g for 10 min to remove the Trypsin, and resuspending the cell pellet to 2.8 ml of cell culture media. The density of the cell suspension was calculated and the whole 2.8 ml of cell suspension cultured to a 25 cm^2 cell bottle with additional 4.2 ml of cell culture media. The cells were sub-cultured like the unDIF cells by the protocol described in section 2.1. The DIF cells were transferred to a 75 cm^2 cell culture bottle on the first following sub-culture day.

2.3 Cell differentiation verification

To verify the HT-29 cell differentiation, the DIF cells were stained with Alcian Blue stain and immunolabelled with antibodies against MUC2 (1 mg/ml, AB11197, Abcam, Netherlands), lysozyme (0.98 mg/ml, ab108508, Abcam, Netherlands), and villin (concentration unknown, ab130751, Abcam, Netherlands). UnDIF cells were used as a control and stained similarly with Alcian blue and immunolabelled with same antibodies.

2.3.1 Alcian Blue staining

The stain was prepared by mixing 80 mg Alcian Blue powder (Hopkin & Williams, United Kingdom) to 80 ml of water. The prepared stain was filtered through 0.2 µm filter (Fisher Scientific) to remove powder clots. The DIF and unDIF HT-29 cells were cultured to glass slips in a density of 30 000 cells per slip and incubated at +37 °C covered in cell media for 3 d. After incubation the cell slips were washed once with PBS. The cells were fixed by putting the slips into +4 °C Methacarn (60% methanol, 30% chloroform, 10% acetic acid) for 15 min on ice. The fixed cells were washed once with 3% acetic acid (97% water, 3% acetic acid). Next, the cells were stained with Alcian Blue stain for 15 min and the excess stain was washed away twice with water. The cell slips were mounted to microscopic slides with Prolong Diamond mountant with DAPI (Invitrogen, USA). The stained DIF and unDIF HT-29 cell slips were imaged with Leica DMi8 (Germany) widefield light microscope. The differentiation was verified by visually estimating if the DIF cells were stained more than the unDIF cells.

2.3.2 Testing with antibodies

The DIF cells should express more MUC2 than the unDIF cells (Centonze et al 2022). MUC2 was tested with immunolabelling following the protocol of Karvonen and colleagues (2021). Shortly, the DIF and unDIF HT-29 cells were cultured to glass slips in a density of 30 000 cells per slip and incubated at +37 °C for 1 d. After incubation the cells were washed twice with 500 µl of PBS. The cells were fixed with 4% paraformaldehyde (500 µl) for 30 min in room temperature (RT) and then washed twice with 500 µl of PBS. After the washes, free aldehydes were blocked with 0.15% glycine in PBS (500 µl) and incubated for 10 min in RT. To permeabilize and block any unspecific binding, 500 µl of Triton solution (0.1% Triton X-100, 0.01% NaN_3 and 2% BSA in PBS) was added onto the slips and incubated for 20 min in RT. The Triton solution was aspirated away and 30 µl of primary antibody (MUC2 1:1500) was pipetted onto the slips and incubated in RT in the dark for 1 h. The slips were washed three times (á 5 min each) with 500 µl of PBS in the dark. The PBS was aspirated away and 30 µl of secondary antibody (anti-mouse 488 antibody 1:200) was pipetted onto the slips and incubated for 30 min in the dark in RT. The cells were washed twice (á 5 min each) with 500 µl of PBS in the dark. The slips were mounted onto microscopic slides

with Prolong Gold with DAPI. The slides were imaged with Leica TCS SP8X Falcon (Germany) confocal microscope and the number of cells with MUC2 were calculated.

Villin and lysozyme antibodies were tested using Western blot method. One sample of 50 000 cells and one sample of 100 000 cells from both DIF and unDIF cells were prepared by mixing the cell suspension with 4x Laemmli and water. The samples were heated for 5 min at +99.0 °C before loading into a 15-well Mini-PROTEAN TGX Stain-free gel (Bio Rad, USA) along with Precision plus protein standards kaleidoscope molecular weight marker (Bio-Rad), 10 µl per well. The gel was run in a Mini-PROTEAN Tetra cell electrophoresis chamber (Bio Rad) at 100 V for 10 min and then at 150 V for 50 min. The gel was activated with UV light in ChemiDoc™ MP Imaging system (Bio Rad) to visualise total protein amount on the gel. The proteins were transferred from the gel with Trans-Blot Turbo Transfer Pack midi-format (Bio-Rad) according to manufacturer's instructions in Trans-Blot Turbo transfer system (Bio Rad). The total protein amount of the blot was visualised with Chemidoc™. Non-specific binding sites were blocked by incubating the blot in 5% BSA in 0.05% tween-TBS at +4 °C on a tube roller overnight.

The next day, the blot was immuno-stained. The primary antibodies were diluted in 5% BSA in 0.05% tween-TBS in 1:50 000 dilution for lysozyme, and 1:1000 dilution for villin. The antibodies were pipetted onto the blot and incubated for 1 h in RT on a platform shaker. The primary antibodies were washed away three times (á 5 min each) with 0.05% TBS-tween on the platform shaker. Secondary antibody (anti-rabbit HRP 1:3000) was pipetted on the blot and incubated for 1 h in RT on a plate rocker. The secondary antibody was washed away five times (á 5 min each) with 0.05% TBS-tween and once for 5 min with TBS without tween. The antibody bands were revealed by adding SuperSignal West Pico PLUS chemiluminescent substrate (Thermo Scientific) and incubating for 5 min in the dark. Excess liquid was blotted away, and the antibody blot imaged with Chemidoc™.

2.4 Virus infection dose test

To test the suitable virus infection dose, the DIF and unDIF HT-29 cells were infected with coxsackievirus A9 (CVA9, 1.94×10^7 pfu/ml, VR-1311 Griggs-strain, ATCC) in different doses. The cells were cultured on glass slips in a density of 15 000 cells per slip. The slips were incubated for 2 d at +37 °C. The tested multiplicity of infection (MOI) doses for the virus were MOI 200, MOI 100, MOI 50, MOI 20, MOI 10, and MOI 1. The prepared infection doses were pipetted onto the cells in glass slips and incubated for 5.5 h at +37 °C. After incubation the cells were immunolabelled as mentioned before (Section 2.3.2). The primary antibodies that were used were 861 rabbit serum antibody (1:1500) and tubulin mouse antibody (1:1500), and the secondary antibodies were anti-rabbit 546

antibody (1:200) and anti-mouse 488 antibody (1:200). The slides were imaged with Leica TCS SP8X Falcon confocal microscope.

2.5 Bacterial infection dose and infection time test

For investigation of the suitable bacterial infection dose and infection time, the DIF and unDIF HT-29 cells were infected with *P. aeruginosa* strain PA14 (10^9 cfu/ml, DSM 19882, DSMZ, Germany) in different doses. The cells were cultured in a 96-well plate in a density of 20 000 cells per well and incubated for 2 d at +37 °C. Before the analysis, the bacterium was grown in LB-agar plate. Colonies were taken from the agar plate, transferred into liquid LB-medium and this liquid bacterial growth was incubated on a shaker at +37 °C overnight. After incubation the bacterial medium was centrifuged for 10 min at 15871 x g and resuspended to 2 ml of PBS. The undiluted PBS-bacterium suspension along with dilutions of 1:2, 1:3, 1:5, and 1:10 were pipetted into a 96-well plate and with Multiskan plate reader (Thermo Scientific, Japan) their optical density (OD) was measured at 495 nm. The dilution with the OD-value closest to 0.5 (containing thus ~1 x 10^6 bacteria) was selected as the sample from which the infection dose dilutions were made. The cells were infected with bacterial infection doses of 10^3 (1000), 10^2 (100), 10^1 (10), 10^0 (1), 10^{-1} (0), and 10^{-2} (-1 bacteria). The tested infection times were 3 h, 5.5 h, and 1 d.

The infected cells were incubated at +37 °C for the selected times. In the 1 d infection the bacterium was on the cells the whole incubation time. After the 3 h and 5.5 h infection times the bacterium was washed away with PBS, fresh cell culture media without GlutaMax and penicillin/streptomycin antibiotic was added to the wells, and the plates were further incubated overnight at +37 °C. After incubation, the possible infection was confirmed by estimating the cytopathic effect (CPE) visually with microscope and by CPE analysis.

CPE analysis was done based on a method by Givirovskaia and colleagues (2022). Briefly, the plate was washed twice with 100 µl of PBS, stained with 50 µl of CPE stain (0.03% crystal violet, 2% ethanol, 36.5% formaldehyde), washed twice with 100 µl of water and lysed with 100 µl of lysis buffer (0.8979 g sodium citrate, 1M HCl in 47.5% ethanol). The absorbance of the plate was measured with Victor x4 2030 multilabel reader (PerkinElmer, USA) at 570 nm using PerkinElmer 2030 manager-software. Each infection dose was also cultured to an LB-agar plate to determine the real number of bacteria in the theoretically estimated infection doses. The agar plates were incubated overnight at +37 °C and the number of colonies were counted.

2.6 Infection test with different viruses

For examination of the infection capability of different viruses against the HT-29 cell line, the cells were infected with CVB3 ($3.45x10^{10}$ pfu/ml, VR-30 Nancy-strain,

ATCC), OC43 (7.43 x 10^7 pfu/ml, hCoV-OC43 VR-1558, ATCC), and formerly used CVA9. The used infection doses were MOI 10, MOI 5, MOI 1, and MOI 0.5 for CVB3 and CVA9, and MOI 100, MOI 50, MOI 20, MOI 10, MOI 5, MOI 1, and MOI 0.5 for OC43. The DIF and unDIF cells were cultured in a 96-well plate in a density of 20 000 cells per well and incubated for 1 d at +37 °C. After incubation, the cells were infected with different doses of the three different viruses and incubated at +37 °C (CVB3 and CVA9) and at +34 °C (OC43). The infection time for CVB3 and CVA9 was 1 d and 3 d, and the OC43 infection time was 5 d. After the incubations the cytopathic effect of possible infection was estimated visually with microscope and by CPE analysis similarly as mentioned in Section 2.5.

2.7 Infection test with different bacteria

To test the infection capability of different bacteria against the HT-29 cell line, the cells were infected with *Pseudomonas aeruginosa* 573 (from Dr. Nina Chanisvili, Eliava institute of bacteriophage, Georgia), *Salmonella enterica* serovar *typhimurium* DS88 (from Prof. Dennis Bamford, University of Helsinki, Finland), *Streptococcus mutans* OMZ381 (from D'Herelle reference centre for bacterial viruses, University of Laval, Quebec, Canada), and *Acinetobacter baumannii* AC54 (from D'Herelle reference centre for bacterial viruses, University of Laval, Quebec, Canada), and formerly used *Pseudomonas aeruginosa* PA14. Before the test, the bacteria were grown in LB-agar plates. Colonies were taken from the agar plates, transferred into liquid LB-medium and this liquid bacterial growth was incubated at +37 °C on a shaker overnight.

After incubation, the liquid medium was centrifuged at 15871 x g for 10 min and resuspended to 2 ml of PBS. The undiluted bacterium-PBS suspensions along with dilutions of 1:2, 1:3, 1:5, and 1:10 were pipetted into a 96-well plate and their optical density (OD) was measured with Multiskan plate reader at 495 nm. The dilution that was closest to OD-value 0.5 (containing thus ~1 x 10^6 bacteria) was chosen for the sample, from which the infection dose dilutions were made. The used infection doses were 10^3 (1000), 10^2 (100), 10^1 (10), 10^0 (1), 10^{-1} (0), and 10^{-2} (-1 bacteria).

The DIF and unDIF HT-29 cells were cultured in a 96-well plate, one plate per bacterium, in a density of 20 000 cells per well and incubated for 2 d at +37 °C. After incubation, the cells were infected with the chosen bacteria in four replicates per dose and incubated at +37 °C for 5.5 h, 1 d and 3 d. After the incubations, the cytopathic effect of possible infection was estimated visually by microscope and by CPE analysis similarly as mentioned in Section 2.5. The infection doses were also cultured to LB-agar plates to define the real number of bacteria in the doses. The plates were incubated at +37 °C overnight, and grown colonies were counted from the plates. Before the CPE analysis was started for the 3 d infection test plates, samples of the four strongest infection doses were taken from two replicate wells per dose on the 96-well plates from each bacterium, except for the *P. aeruginosa* PA14 and 100 µl of each sample was cultured to an

LB-agar plate. The plates were incubated overnight at +37 °C. This was done to estimate the viability of the bacteria after the 3 d incubation period.

2.8 Infection test with CVA9 and MUC2 antibody

To test whether the mucus produced by the mucus-producing cells protects the cells from viral infection, the cells were infected with CVA9 enterovirus and labelled with MUC2 antibody, a biomarker for the mucus. The DIF and unDIF HT-29 cells were cultured on glass cover slips in a density of 30 000 cells per slip, and incubated overnight at +37 °C. The cells were infected for 5.5 h with CVA9 with an infection dose of MOI 1. After the infection, the infected cells were immunolabelled similarly as mentioned in Section 2.3.2. The primary antibodies used were MUC2 (1:1000) and 861 rabbit serum (1:1500). The secondary antibodies used were anti-mouse 488 (1:200) and anti-rabbit 546 (1:200). The slips were imaged with Leica TCS SP8X Falcon confocal microscope with Leica Application Suite X (LAS X) program.

2.9 Imaging with confocal microscope

The virus infection dose test samples, MUC2 antibody testing samples, and samples of cells infected with CVA9 and labelled with MUC2 were imaged with Leica TCS SP8X Falcon confocal microscope with Leica Application Suite X (LAS X) program. The used lasers were 405 nm diode laser and white light laser, the used objective was HC PL APO CS2 63x/1.30 glycerol, speed 600, and format 512 x 512. The used fluorescent labels were DAPI, Alexa 546, and Alexa 488. The samples were imaged as stacks.

2.10 Image analysis

The confocal microscope images were analysed with Image J software (National institutes of health, USA). The images were converted to 8-bit and the stack signal was combined with Max intensity. The Lookup table (LUT) was changed to HiLo before adjusting the brightness/contrast to exclude the background, and 0.5 Gaussian blur filter was used. The cell nucleus (blue), tubulin (green), virus (red), and MUC antibody (yellow) were all coloured with different LUTs for better visualisation.

2.11 Data analysis with GraphPad

The CPE analysis' absorbance results were analysed with GraphPad Software Inc. (USA). The chosen graph type was column bar graph where the mean was plotted with Standard Error of the Mean (SEM). An average was calculated from

the replicate values of each infection dose, and they were normalised against the average of cell control replicates. The normalised values were analysed with Two-way ANOVA with multiple comparisons. Multiple comparisons were corrected with Bonferroni methods. P-values <0.05 were considered statistically significant.

3 RESULTS

3.1 Verification of cell differentiation

For verification of the differentiation of the HT-29 cells to mucus-producing DIF HT-29 cells after the eight-day differentiation protocol, the DIF and unDIF cells were stained with Alcian blue and imaged with a widefield light microscope. Alcian blue is a histochemical stain that attaches to the acidic muco-substances or mucopolysaccharides of the mucins that the mucus-producing cells produce (Limage et al. 2020). The DIF cells stained blue, verifying that the cells had differentiated, as Alcian Blue had stained the mucus the DIF cells produced (Figure 1B). In Figure 1A are the unstained DIF cells as negative control. Alcian blue did not stain unDIF HT-29 cells which remained colourless, or the staining was only visible in a few cells (Figure 1D). In Figure 1C are the unstained unDIF cells as negative control.

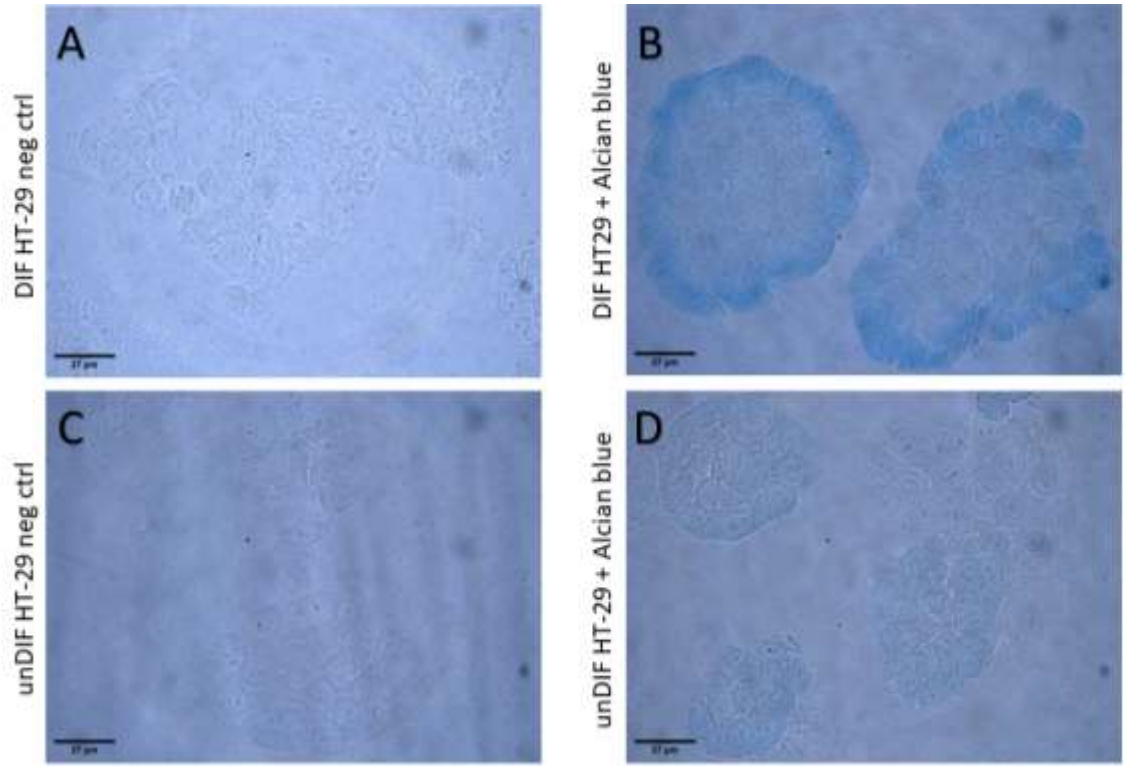

Figure 1. Alcian blue stain verified the successful cell differentiation. The unDIF (undifferentiated) and DIF (differentiated) HT-29 cells were stained with Alcian blue stain to verify that the cell differentiation protocol had differentiated the cells into mucus producing cells. Unstained DIF (A) and unDIF cells (C) were a negative control. Alcian blue stained the mucus of the DIF cells blue (B), verifying the differentiation to mucus-producing cells. Alcian blue did not dye the unDIF cells (D) as they do not produce mucus to attach to. Scale bar 27 µm.

To assess whether the DIF cells expressed more MUC2 than the unDIF cells, the DIF and unDIF cells were labelled with MUC2 antibody and imaged with confocal microscope. MUC2 antibody attaches to the major colonic mucin MUC2 secreted by the mucus-producing cells (Leteurtre et al. 2004). Figure 2 illustrates the images of MUC2-labelled cells from which the number of cells expressing the MUC2 was counted. The MUC2 expression was weak in both DIF and unDIF HT-29 cells and there was no difference in the number of MUC2 expressing cells between the DIF and unDIF HT-29 cells (Table 1).

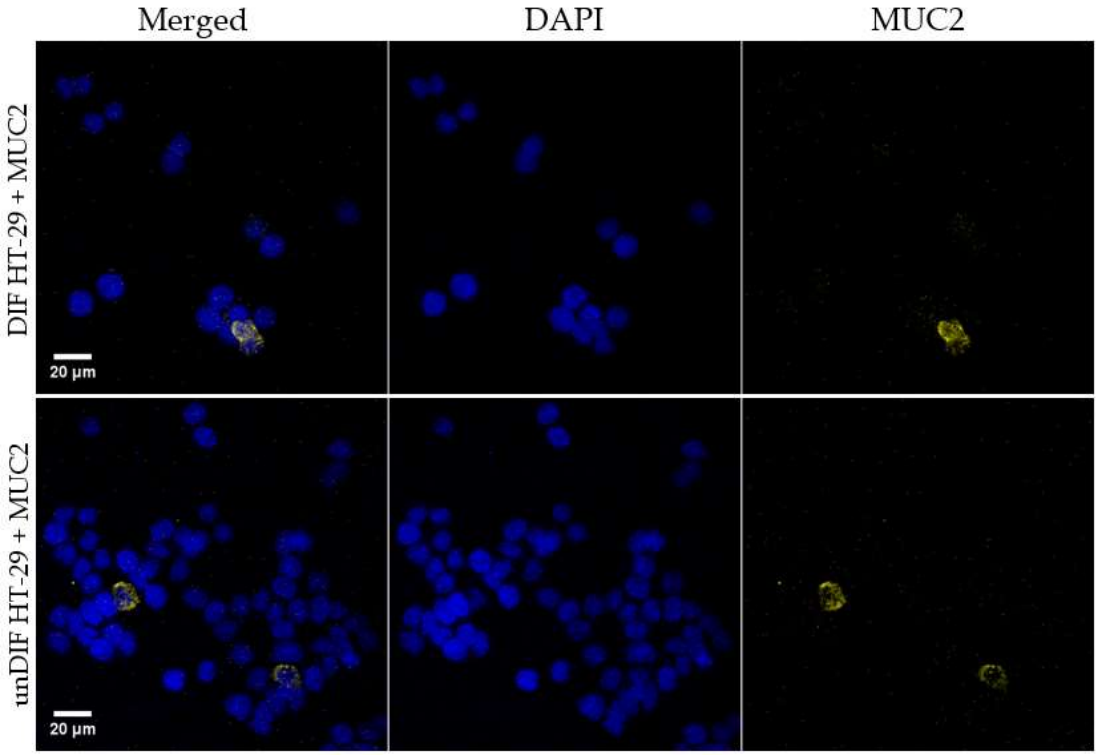

Figure 2. Difference in MUC2 expression was not detected between the DIF (differentiated) and unDIF (undifferentiated) cells. The DIF and unDIF HT-29 cells were labelled with MUC2 (1:1500) to test if the DIF cells express more MUC2 than the unDIF cells. The images are represented in merged images of DAPI (blue, nucleus) and MUC (yellow) with a 20 µm scale bar, as well as individual images of both labels.

Table 1. MUC2 expression was equally low in both the DIF (differentiated) and unDIF (undifferentiated) HT-29 cells. From the confocal microscope images, ~100 DIF and unDIF HT-29 cells were calculated and the percentage of MUC2 expressing cells (MUC+) calculated from the total cell count. The DIF cells should express more MUC2. The MUC2 expression was 1.9% in both cell types and thus did not verify the successful differentiation.

Cell type	Total cell count	MUC+	MUC-
DIF HT-29	104	2 (1.9%)	102 (98.1%)
unDIF HT-29	107	2 (1.9%)	105 (98.1%)

For further cell differentiation verification, the DIF HT-29 cells and unDIF HT-29 cells were tested with villin and lysozyme antibodies with Western blot. There was no significant difference between the DIF and unDIF HT-29 cells in either villin or lysozyme expression (Figure 3). There was a difference between the lysozyme expression in the lower cell density, but as this analysis was not replicated, the difference could have resulted from a pipetting error or some other artefact. Therefore, the expression of these antibodies did not confirm the successful cell differentiation.

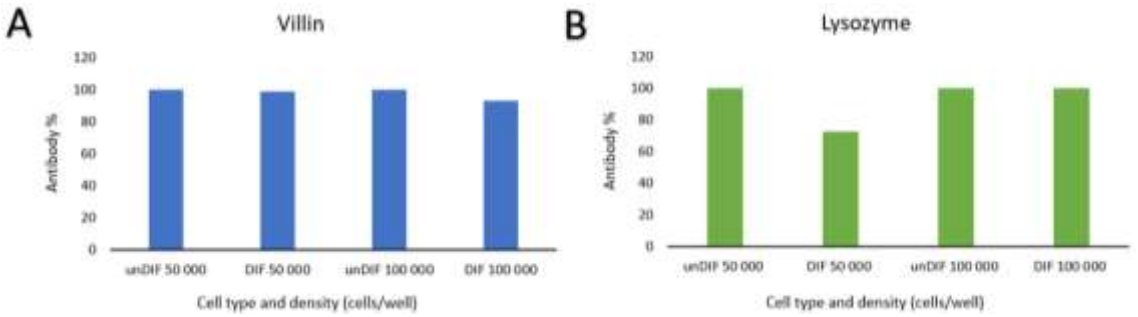

Figure 3. Villin and lysozyme antibody expression did not confirm successful HT-29 cell differentiation. The DIF (differentiated) and unDIF (undifferentiated) HT-29 cells were tested with villin and lysozyme antibodies in cell densities of 50 000 cells and 100 000 cells. Villin expression did not differ between the cell types in either cell density (A). DIF HT-29 cells expressed less lysozyme in a cell density of 50 000 (B), but this could result from a laboratory error as the analysis was performed only once.

3.2 Virus infection dose test

The suitable viral infection dose was tested by infecting the DIF and unDIF HT-29 cells with CVA9 using MOIs 200, 100, 50, 20, 10, and 1. The suitable infection would be close to 50% to better observe the changes in the possible various following and future analyses. Infectivity close to 100% was unwanted, because the course of infection is not suitable to study if all the cells are infected and therefore, dead. The three largest infection doses resulted in overly infected samples and were thus excluded from future analyses. Figures 4 and 5 demonstrate the microscope images of the infected DIF and unDIF cells, respectively, in three smallest infection doses and from these images the number of infected and uninfected cells were counted. MOI 20 and MOI 10 were excessively strong as both doses infected >84% of the cells while MOI 1 infected ~70% of the cells (Table 2). The infection was 3-5% stronger in MOI 10 and MOI 1, and 15% stronger in MOI 20 in the unDIF cells. The aim for the suitable infection dose was ~50% and thus, MOI 1 was selected for future analyses.

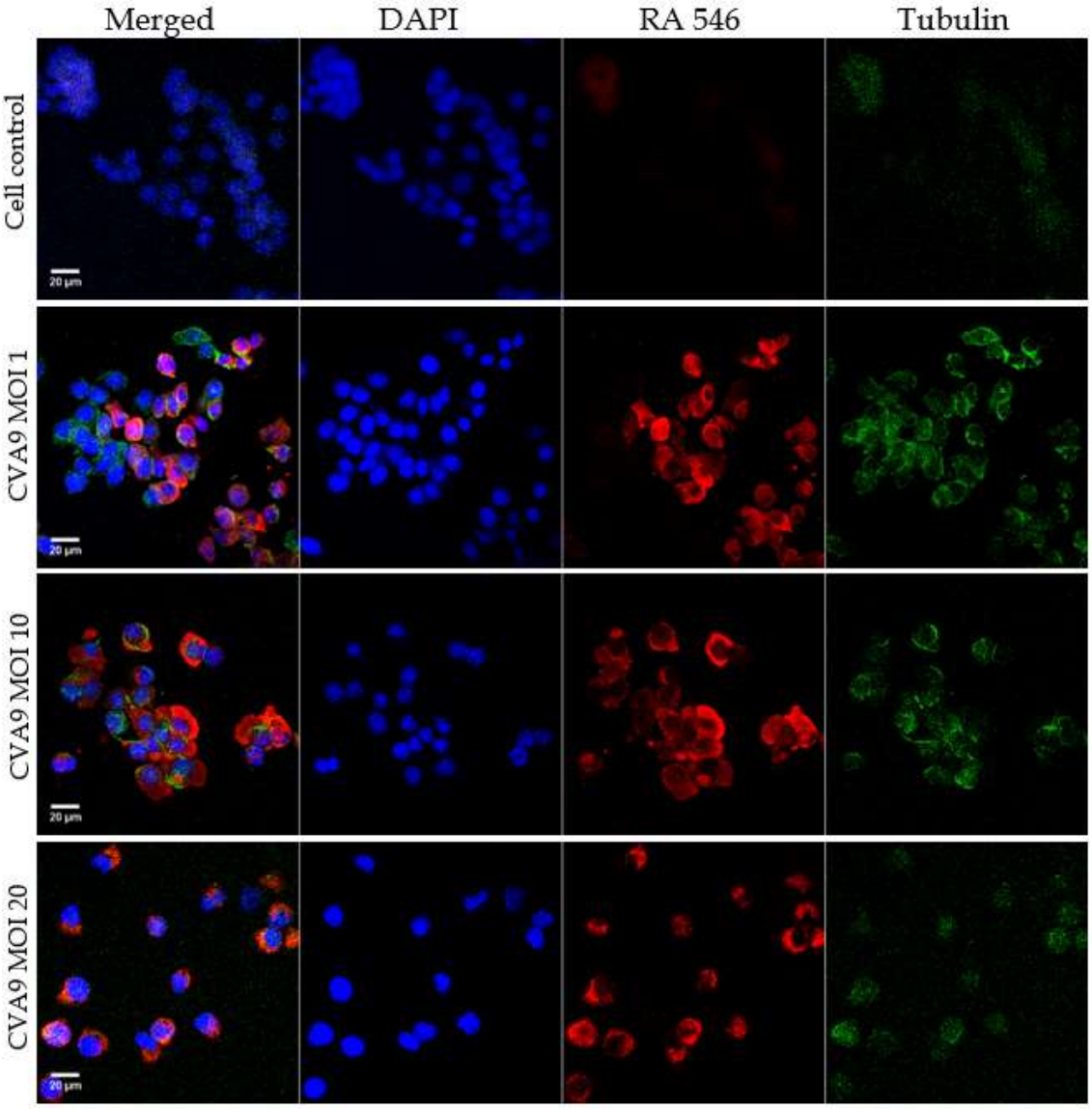

Figure 4. CVA9 dose MOI 1 was the suitable infection dose. The differentiated HT-29 cells were infected with CVA9 doses MOI 20, MOI 10, and MOI 1 to find the most suitable infection dose. Illustrative confocal images of different doses are represented in merged images of DAPI (blue, nucleus), RA546 (red, virus), and tubulin (green) with a scale bar of 20 µm, as well as individual images of each label. By counting the number of infected cells from the images, MOI 1 was selected as the most suitable dose.

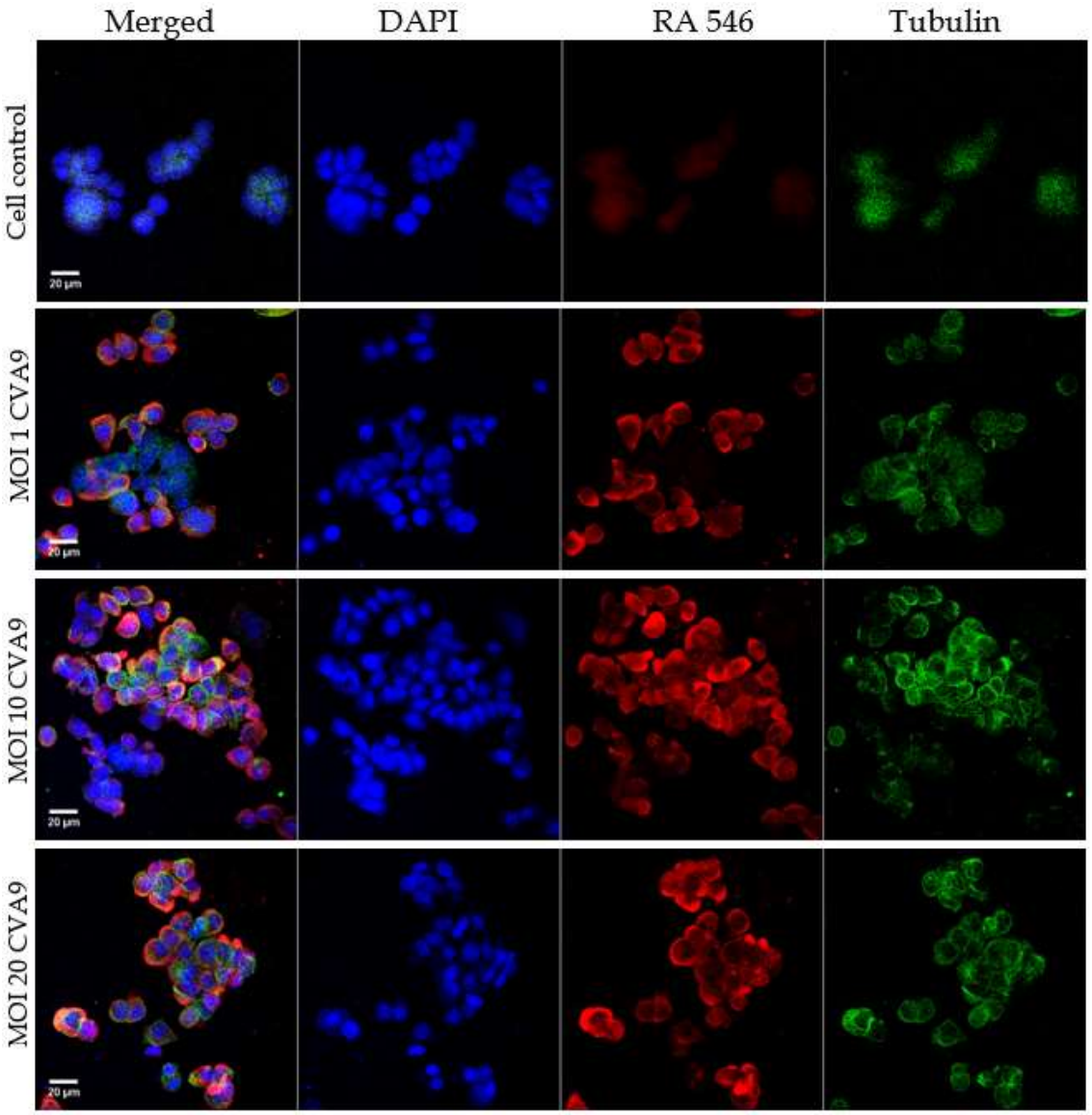

Figure 5. MOI 1 infection dose of CVA9 was the suitable infection dose. To find the most suitable infection dose, the undifferentiated HT-29 cells were infected with CVA9 doses MOI 20, MOI 10, and MOI 1. The confocal microscope illustrative images of different infection doses are displayed in merged images of DAPI (blue, nucleus), RA546 (red, virus), and tubulin (green) with a 20 µm scale bar, along with individual images of each label. The infected cells were counted from the images, resulting in the selection of MOI 1 as the most suitable infection dose.

Table 2. The number of CVA9 infected cells at different MOIs. The number and percentage of infected and uninfected DIF (differentiated) and unDIF (undifferentiated) HT-29 cells were calculated from the confocal microscope images of the CVA9 doses MOI 20, MOI 10, and MOI 1. The percentage of infected cells in MOI 20 and MOI 10 was too high, but the percentage in MOI 1 was optimal and was therefore utilised in future experiments.

Cell type and virus dose	Total cell number	Infected cells	Uninfected cells
DIF HT-29 MOI 1	132	68 (52%)	64 (48%)
DIF HT-29 MOI 10	98	85 (87%)	13 (13%)
DIF HT-29 MOI 20	104	84 (81%)	20 (19%)
unDIF HT-29 MOI 1	129	73 (57%)	56 (43%)
unDIF HT-29 MOI 10	98	88 (90%)	10 (10%)
unDIF HT-29 MOI 20	102	97 (95%)	5 (5%)

3.3 Bacterial infection dose and infection time test

To test the suitable bacterial infection dose and infection time, DIF and unDIF cells were infected with *P. aeruginosa* PA14. The lowest tested infection time was 3 h, which was not enough for the infection to occur, and thus this infection time was not chosen for further use. The longest tested infection time was 1 d which was excessively long, as all infection doses lead to 80% cell death (Figure 6) and therefore this infection time was not chosen either. The most suitable infection time seemed to be 5.5 h, since the cell viability significantly reduced in the two strongest doses (two-way ANOVA DIF HT-29 cells $F_{6, 18} = 80.13$, df = 6, $p<0.0001$, unDIF HT-29 cells $F_{6, 18} = 57.35$, df = 6, $p<0.0001$) but most of the cells survived in the lower doses. In pairwise comparisons, the two strongest infection doses significantly differed from the cell control (p-values Bonferroni corrected) (Figure 7).

The effect of the penicillin + streptomycin antibiotic in the cell culture medium on the bacterial infection was also tested with the 5.5 h infection test. The medium with antibiotics prevented the infection from happening in all infection doses while the infection occurred in the two strongest infection doses in a medium without antibiotics, as mentioned earlier. When counting the colonies from the LB-agar plates, it was noticed that the infection doses were 10x stronger than theoretically was estimated. However, the result images were made using the theoretical infection doses.

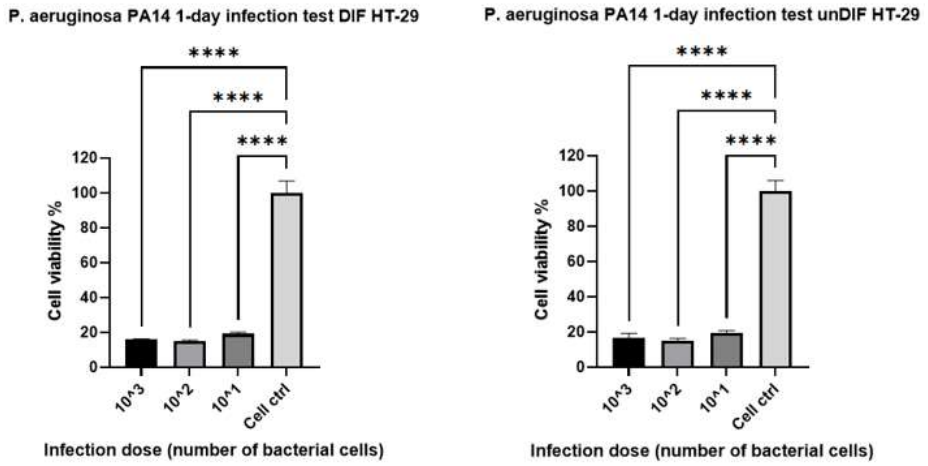

Figure 6. Cell viability reduced in excess in *P. aeruginosa* PA14 1 d infection test. The DIF (differentiated) and unDIF (undifferentiated) HT-29 cells were infected with *P. aeruginosa* PA14 in different infection doses for 1 d. The infection was strong in all infection doses reducing the cell viability >80%. The mean values of each infection dose were normalised against the cell control. Two-way ANOVA and Bonferroni post hoc tests were done between the different doses and the cell control (p=0.0001 (****)).

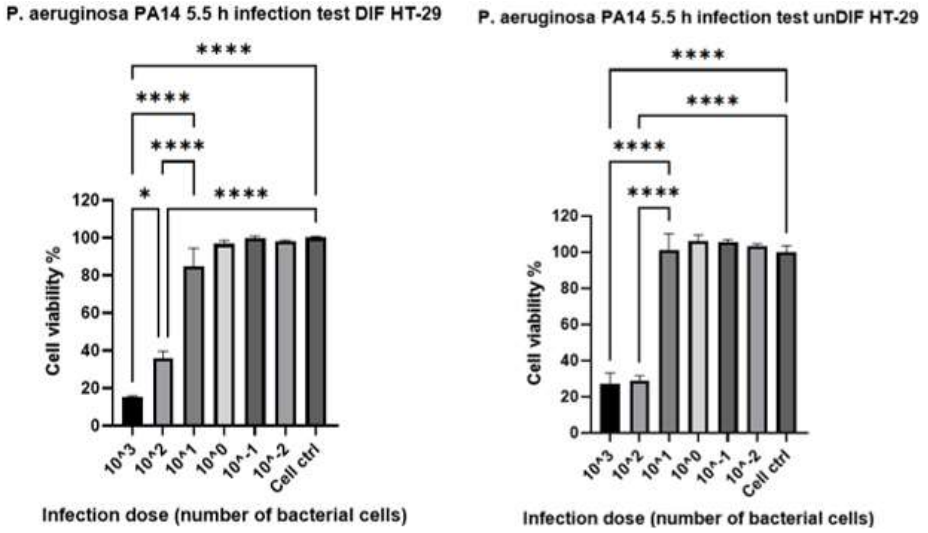

Figure 7. The most suitable infection time for *P. aeruginosa* PA14 infection was 5.5 h. An infection time of 5.5 h with *P. aeruginosa* PA14 was tested on the DIF (differentiated) and unDIF (undifferentiated) HT-29 cells. The cell viability reduced by >50% in the two strongest infection doses, but the majority of cells survived in the lower doses. The mean values of each infection dose were normalised against the cell control. Two-way ANOVA and Bonferroni post hoc tests were executed between the different doses and the cell control (p=<0.0001 (****) and <0.05 (*)).

3.4 Infection test with different viruses

The infectivity of different viruses against the HT-29 cell line was tested by infecting the DIF and unDIF HT-29 cells with CVA9, CVB3 and OC43. CVA9 infected the cells strongly, significantly reducing cell viability by ≥75% both in 3 d infection time (two-way ANOVA DIF HT-29 cells $F_{4, 8} = 929.8$, df = 4, $p < 0.0001$, unDIF HT-29 cells $F_{4, 8} = 801.5$, df = 4, $p<0.0001$), and in 1 d infection time (two-way ANOVA DIF HT-29 cells $F_{4, 8} = 3214$, df = 4, $p<0.0001$, unDIF HT-29 cells $F_{4, 8} = 1076$, df = 4, $p<0.0001$) in all infection doses (Figure 8). Similarly, the infectivity of CVB3 was strong in 3 d infection time, significantly reducing cell viability by ≥75% (two-way ANOVA DIF HT-29 cells $F_{4, 8} = 507.4$, df = 4, $p<0.0001$, unDIF HT-29 cells $F_{4, 8} = 823.3$, df = 4, $p<0.0001$) and also in 1 d infection time (DIF HT-29 cells $F_{4, 8} = 302.9$, df = 4, $p<0.0001$, unDIF HT-29 cells $F_{4, 8} = 1657$, df = 4, $p<0.0001$) in all infection doses (Figure 9). In pairwise comparisons, all doses significantly differed from the cell control (p-values Bonferroni corrected). OC43 did not infect the DIF or unDIF HT-29 cells in any of the tested infection doses (Figure 10).

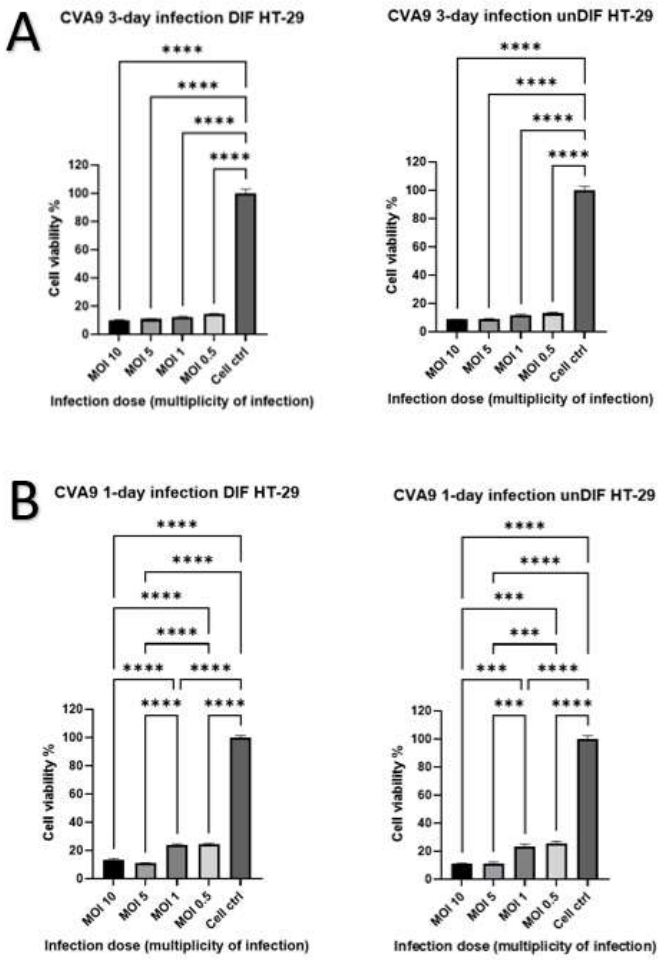

Figure 8. CVA9 1 d infection time was more suitable than the 3 d infection time. The DIF (differentiated) and unDIF (undifferentiated) HT-29 cells were infected with different CVA9 infection doses for 3 d (A) and for 1 d (B). Both infection times and all infection doses infected the cells strongly, reducing cell viability by >75%. The mean values of each infection dose were normalised against the cell control. Two-way ANOVA and Bonferroni post hoc tests were done between the different doses and cell control (p=<0.0001 (****) and <0.001 (***)).

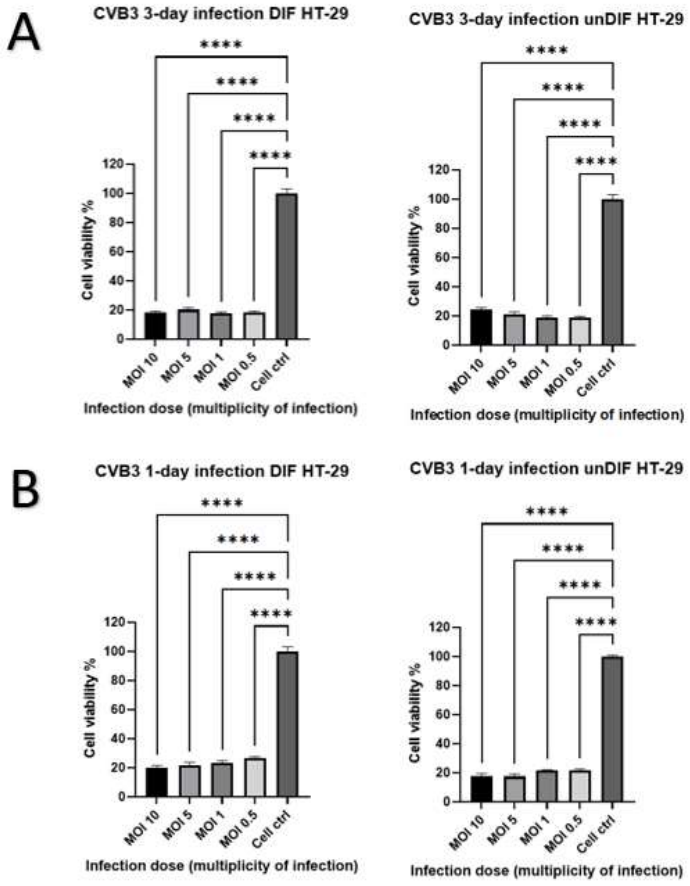

Figure 9. The 1 d infection time was more suitable for CVB3 than the 3 d infection time. CVB3 infectivity was tested on the DIF (differentiated) and unDIF (undifferentiated) HT-29 cells with different infection doses for 3 d (A) and 1 d (B). All infection doses infected the cells strongly in both infection times, reducing the cell viability by >70%. The mean values of each infection dose were normalised against the cell control. Two-way ANOVA and Bonferroni post hoc tests were done between the different doses and cell control (p=<0.0001 (****)).

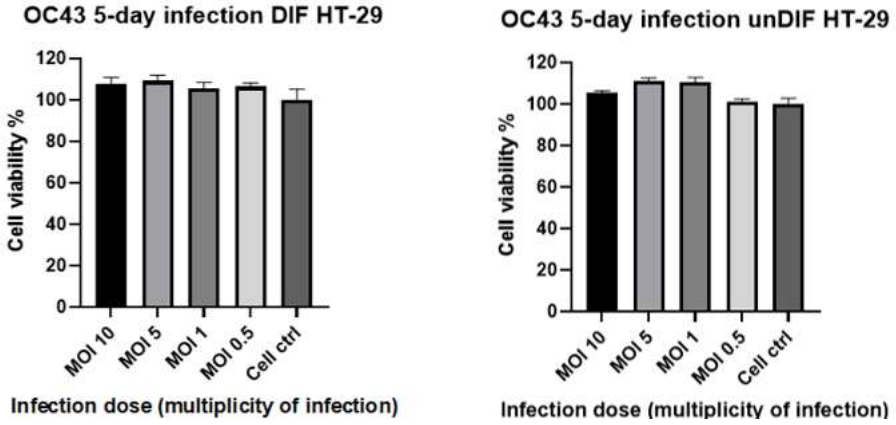

Figure 10. OC43 did not infect the HT-29 cells. A 5 d infection with OC43 was tested on the (DIF) differentiated and unDIF (undifferentiated) cells with various infection doses. Infection did not occur at any infection dose. The mean values of each infection dose were normalised against the cell control. Two-way ANOVA and Bonferroni post hoc tests were done between the different doses and cell control. There were no statistically significant differences.

3.5 Infection test with different bacteria

To examine the ability of different bacteria to infect the HT-29 cell line, the DIF and unDIF HT-29 cells were infected with *P. aeruginosa* 573, *S. typhimurium* DS88, *Str. mutans* OMZ381, *A. baumannii* AC54, and *P. aeruginosa* PA14. From the tested infection times, the 5.5 h and 1 d infection times were not enough for the infection to occur in any of the tested bacteria, except with *P. aeruginosa* PA14, which was already tested on the cells beforehand and its infectivity within 5.5 h was known. After the 3 d infection time, clear infection occurred in both *P. aeruginosa* strains. The infection was visible with microscopical observation and in the CPE plate before lysis of the cells. However, due to the probable biofilm formation to which the CPE stain attached to (Figure 11A), the effect of infection could not be detected when the cells, and simultaneously the biofilms, were lysed in the CPE analysis (Figure 11B). Because of these reasons, the results and significance of cell viability did not correspond to the reality of the infection strength, and the infection appeared as non-existent or only mild (Figure 12).

The cell viability results of the 3 d infection of *S. typhimurium, Str. mutans*, and *A. baumannii* are presented in Figure 13. *S. typhimurium* indicated a mild infection in the two strongest doses for DIF HT-29 cells and significantly reduced cell viability by ~20% (two-way ANOVA $F_{6, 18} = 7.380$, df = 6, $p<0.0004$) in the strongest infection dose. In the unDIF HT-29 cells, *S. typhimurium* significantly infected the cells in the three strongest infection doses (two-way ANOVA $F_{6, 18} = 50.28$, df = 6, $p<0.0001$), reducing the cell viability by ~30% in the strongest, ~20% in the second strongest, and ~15% in the third strongest infection dose. In

pairwise comparisons, the strongest infection dose in DIF HT-29 cells and the three strongest infection doses in unDIF HT-29 cells significantly differed from the cell control (p-values Bonferroni corrected). *Str. mutans* did not infect the DIF HT-29 cells, but mildly infected the unDIF HT-29 cells in the three strongest doses, significantly reducing cell viability (two-way ANOVA $F_{6, 18} = 21.63$, df = 6, $p<0.0001$) by ~25% in the two strongest infection doses, and by ~20% in the third strongest infection dose. In pairwise comparisons, the three strongest infection doses significantly differed from the cell control (p-values Bonferroni corrected). *A. baumannii* was not able to infect the cells even after the 3 d incubation.

When the colonies were counted from the agar plates that were cultured first, it was noted that the *P. aeruginosa* PA14 and *S. typhimurium* infection doses were ~10x stronger than theoretically estimated. With *P. aeruginosa, Str. mutans* and *A. baumannii* the two mildest infection doses were as theoretically estimated, but the infection doses from 10^0 to 10^3 were ~10x stronger. However, the result graphs were made using the theoretically estimated infection doses. When the growth was visually inspected from the agar plates that were cultured from the samples that were taken from the 96-well plate after 3 d infection period, it was noticed that other bacteria were still viable and formed colonies on the plates, but *A. baumannii* did not grow on the plates. Therefore, it was concluded that *A. baumannii* was not viable after the 3 d period on the cells and thus, no infection occurred.

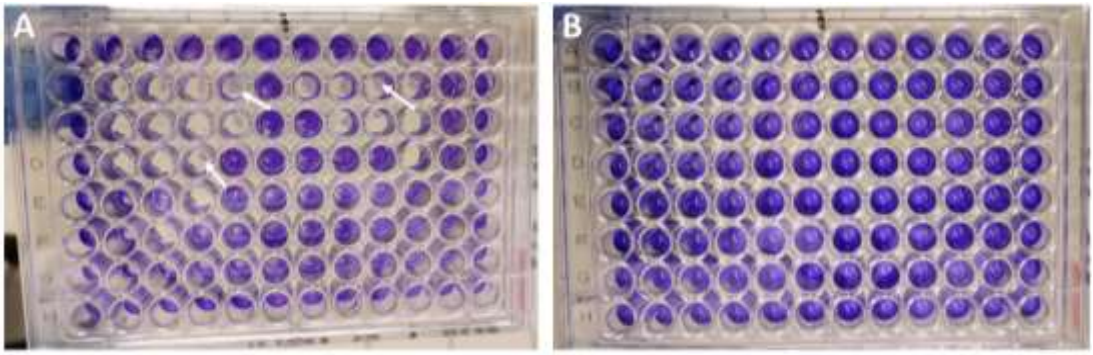

Figure 11. *P. aeruginosa* 573 formed biofilms (white arrows) during the 3 d infection. The DIF (differentiated) and unDIF (undifferentiated) HT-29 cells were infected with *P. aeruginosa* 573 for 3 d. The bacterium infected the cells and detached the cells from the bottom of the well but formed biofilms (A), to which the CPE stain attached. When the cells were lysed, the biofilm released the stain (B), and the absorbance of the wells did not resemble the reality of the infection.

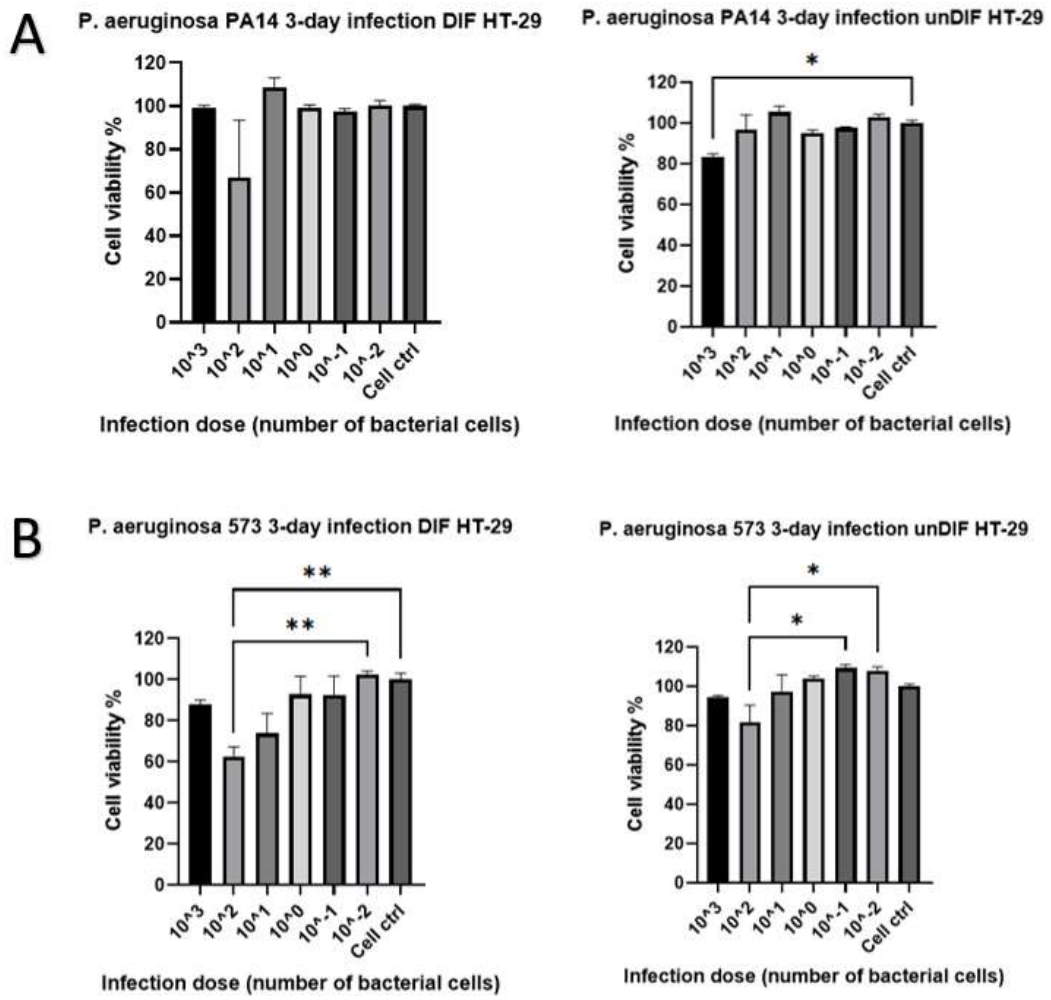

Figure 12. Both *P. aeruginosa* strains infected the cells during the 3 d infection test. The DIF (differentiated) and unDIF (undifferentiated) HT-29 cells were infected with *P. aeruginosa* PA14 and *P. aeruginosa* 573 in different infection doses for 3 d. Both bacteria infected the cells, but due to biofilm formation and the CPE stain dying the biofilm, the cell viability results did not correspond to the infection strength, distorting the results. The mean values of each infection dose were normalised against the cell control. Two-way ANOVA and Bonferroni post hoc tests were done between the different doses and cell control ($p=<0.01$ (**) and <0.05 (*)).

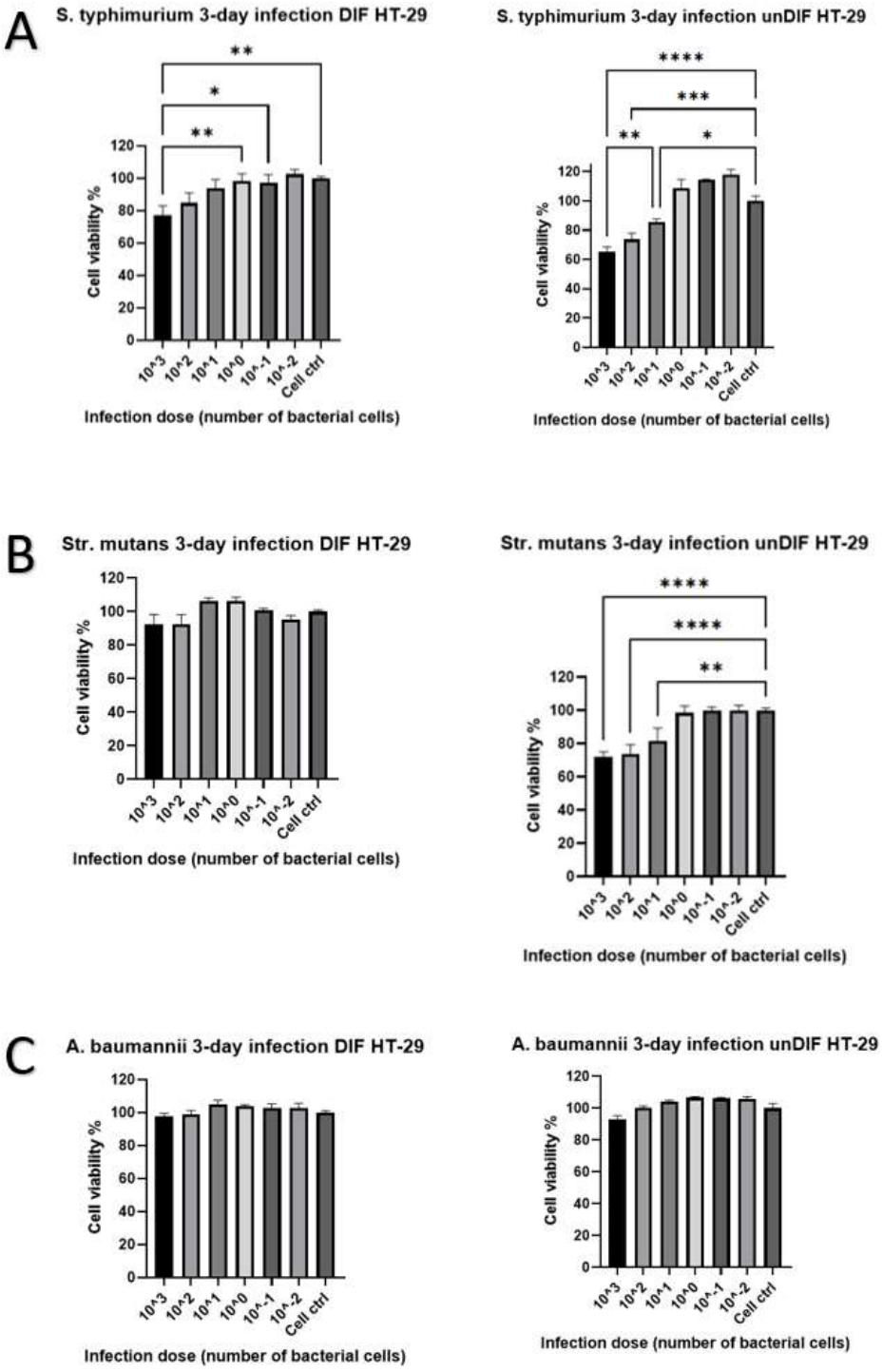

Figure 13. A mild infection occurred after 3 d infection time with *S. typhimurium* and *Str. mutans,* but *A. baumannii* did not infect the cells. The DIF (differentiated) HT-29 cells and unDIF (undifferentiated) HT-29 cells were infected with the three bacteria species in different infection doses for 3 d. *S. typhimurium* infected both cell types mildly, reducing cell viability by ~20-30% (A). *Str. mutans* infected only the DIF HT-29 cells mildly, reducing cell viability by ~20-30% (B). *A. baumannii* did not infect the cells (C). The mean values of each infection dose were normalised against the cell control. Two-way ANOVA and Bonferroni post hoc tests were performed between the different doses and the cell control (p=<0.0001 (****), <0.001 (***), <0.01 (**), and <0.05 (*)).

3.6 Infection test with CVA9 and MUC2 antibody

The DIF and unDIF HT-29 cells were infected with CVA9 and labelled with MUC2 antibody to investigate whether the mucus of the cells protects them from infection. MUC2 is a marker used to detect the mucin produced by the mucus-producing cells (Centonze et al. 2022). The number of uninfected cells, uninfected cells with MUC2, infected cells without MUC2, and infected cells with MUC2 were counted from the confocal microscope images illustrated in Figure 14 (DIF HT-29 cells) and Figure 15 (unDIF HT-29 cells). The number and percentage of the cell counts are presented in Table 3. The presence of mucus did not indicate protection for the cells against infection, as the expression of MUC2 in uninfected cells was 0% in DIF HT-29 cells and 0.9% in unDIF HT-29 cells (Table 3). Meanwhile, the expression of MUC2 in infected cells was 2.6% in DIF HT-29 cells and 1.7% in unDIF HT-29 cells (Table 3).

Interestingly, CVA9 MOI 1 infection dose was 17.7% stronger in the DIF HT-29 cells and 12.7% stronger in the unDIF HT-29 cells here (Table 3) than when originally tested (Table 2). In the original infection dose analysis (Section 3.2) the MOI 1 infection was ~50% but here almost 90% of the cells were infected. The reason for the excessive infectivity is unknown.

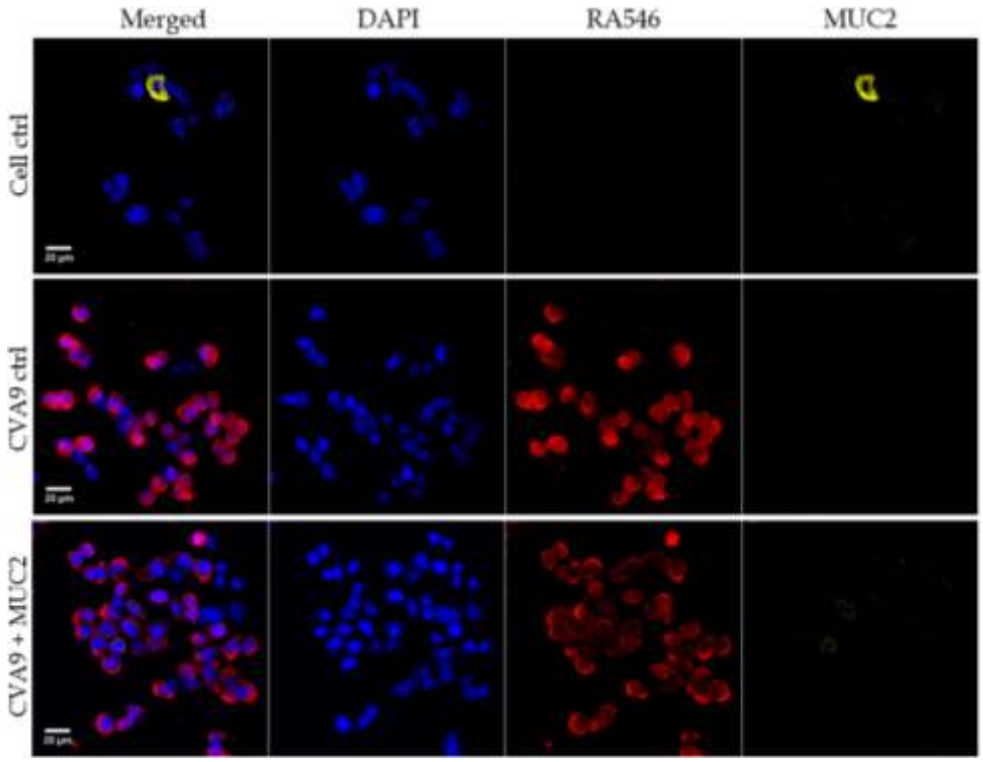

Figure 14. MUC2 expression of the differentiated (DIF) HT-29 cells indicated no mucosal protection of the cells against CVA9 infection. The DIF HT-29 cells were infected with CVA9 and labelled with MUC2 antibody, a marker for mucus production, to examine whether the mucus production of the cells protects the cells from

infection. Illustrative confocal images are represented in merged images of DAPI (blue, nucleus), RA546 (red, virus), and MUC2 (yellow) with a scale bar of 20 µm, as well as individual images of each label.

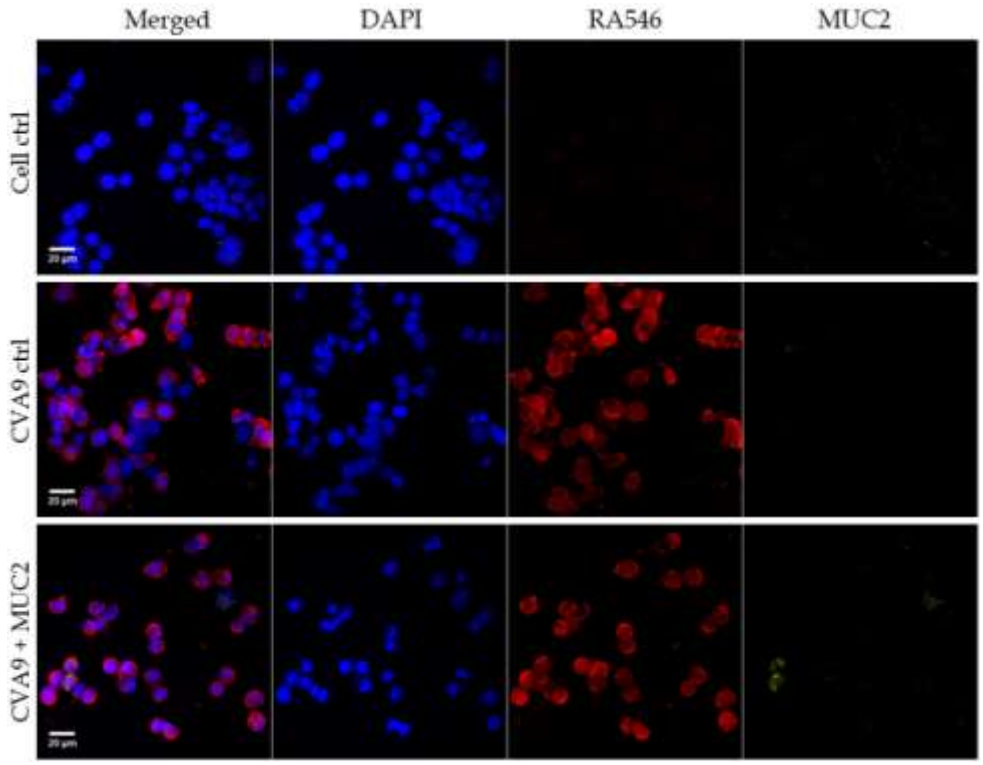

Figure 15. According to MUC2 expression of the unDIF (undifferentiated) HT-29 cells, the mucus did not protect the cells against CVA9 infection. The unDIF HT-29 cells were labelled with MUC2 antibody, a mucus production marker, and infected with CVA9 to assess whether the cells are protected from infection by the mucus they produce. Confocal microscope images are represented in merged images of DAPI (blue, nucleus), RA546 (red, virus), and MUC2 (yellow) with a 20 µm scale bar, as well as individual images of each label.

Table 3. Presence of CVA9 and MUC2 in DIF (differentiated) and unDIF (undifferentiated) HT-29 cells based on antibody labelling. The number and percentage of uninfected cells (Cell only), uninfected cells with MUC2 (Cell + MUC2), CVA9 infected cells (Cell + CVA9), and CVA9 infected cells with MUC2 (Cell + CVA9 + MUC2) were calculated from the confocal microscope images. The mucus, detected with MUC2 antibody, protected neither the DIF HT-29 cells nor the unDIF HT-29 cells from infection.

Cell type	Total cell number	Cell only	Cell + MUC2	Cell + CVA9	Cell + CVA9 + MUC2
DIF HT-29	231	27 (11.7%)	0 (0%)	198 (85.7%)	6 (2.6%)
unDIF HT-29	230	27 (11.7%)	2 (0.9%)	197 (85.7%)	4 (1.7%)

4 DISCUSSION

The aims of this study were to validate the differentiation protocol for the HT-29 cell differentiation to mucus producing cells and to test the suitability of HT-29 cell model as an infection model for future use with the analysed pathogens. The cells were differentiated for eight days on a topographic surface and the differentiation was verified with Alcian blue staining and antibody testing. The infectivity of the investigated pathogens was studied with CPE analysis.

4.1 Differentiation to mucus-producing cells was fast and successful

The HT-29 colorectal adenocarcinoma cells can be differentiated to mucus producing cells on a topographic surface and the mucus produced by the differentiated cells stained with Alcian Blue (Centonze et al. 2022). Alcian blue is a dye that attaches to the mucus, and thus it can be used to detect whether mucus is produced or not (Limage et al. 2020). Therefore, the Alcian blue staining was done for both unDIF and DIF HT-29 cells to see the difference in mucus production, hence confirming the differentiation of the cells. In general, it was noticed that the cells did not grow as individuals or a confluent layer of cells, but as clusters of many cells with space in between the clusters. The unDIF cells contained only a few lightly stained cells but most of the cells did not stain at all (Figure 1D). In contrast, all DIF HT-29 cell clusters stained blue from the outer rim indicating that the cells produced mucus to the edges of the clusters and verifying the successful differentiation (Figure 1B). Furthermore, the unDIF cells should not contain the mucus producing cells and as the Alcian blue did not stain them, it further verified that the differentiation was successful.

There were less stained and unstained cells in the centre of the DIF cell clusters which could indicate that only a certain percent of the cells differentiated to mucus producing cells but not all. This is in agreement with earlier studies where it was observed that the HT-29 cells differentiated on the topographic surface contained both enterocytes and mucus producing goblet cells (Centonze et al. 2022). The unstained cells present in the DIF cell sample were possibly enterocytes which are not mucus producing and thus, lacked Alcian blue stain. In the future, the cell differentiation on the topographic surface could be further studied and verified by investigating the differentiation-associated proteins of the enterocytes and goblet cells as Ferraretto and colleagues (2018) have done, to learn whether both cell types are present in the DIF cells and at what percentage.

The differentiation of the HT-29 cells using this kind of topographic surface is a novel method, pioneered by Centonze and colleagues (2022). Traditionally, the HT-29 cells have been differentiated to mucus-producing cells by exposing

the cells to methotrexate (MTX) for approximately 30 days (Lesuffleur et al. 1990, Centonze et al. 2022). The state of differentiation depends on the concentration of MTX to which the HT-29 cells are exposed to (Martínez-Maqueda et al. 2015). At a lower MTX-concentration, the cells differentiate to a mixed population of enterocytes and mucus-producing goblet cells, whereas at higher concentrations the cells differentiate almost exclusively to goblet cells (Simon-Assmann et al. 2007). When comparing the differentiation on the topographic surface to the differentiation with MTX, the evident advantage of the surface is the short differentiation period. The differentiation can be done in eight days while with MTX it would take up to 30 days (Lesuffleur et al. 1990, Centonze et al. 2022), which considerably shortens the workflow. The costs of differentiation protocol with the surface are also considerably lower as there is no need for expensive reagents. On the contrary, the MTX differentiation is more versatile because the cells can be differentiated to different populations and more abundantly to mucus-producing cells.

4.2 Mucin expression might be more versatile than expected

The antibody tests did not fully confirm successful cell differentiation as there was no difference in the expression of the tested MUC2 (Table 1), villin (Figure 3), and lysozyme (Figure 3) antibodies between the DIF and unDIF cells. MUC2 was used to confirm the differentiation to mucus producing goblet cells, while villin is a biomarker for enterocytes and lysozyme a biomarker to Paneth cells. Centonze and colleagues (2022) did a similar differentiation study with the topographic surface and labelled the cells with MUC2, villin and lysozyme. In their study the cells that were differentiated for eight days, like in this study, contained 2% more MUC2 expressing cells, only about 0.4 % more villin expressing cells, and about 11% more lysozyme expressing cells than the unDIF cells (Centonze et al. 2022). They reflected that the difference in MUC2 expression was considerably low, while the difference in lysozyme expression was surprising, and hypothesised that the lysozyme expression might indicate that the cells had also differentiated to Paneth cells and not only to mucus-producing cells (Centonze et al. 2022).

The results here may not be completely comparable to the study of Centonze and colleagues, because in this study villin and lysozyme were tested with another method. The immunolabelling of villin and lysozyme was not successful, and therefore these antibodies were tested with Western blot instead (Figure 3). Hence, though Centonze et al (2022) detected an 11% difference in lysozyme expression that was not detected here, it could result from the difference of used methods.

There is a possibility that the cells were differentiated, but they express some other mucin than MUC2. The several other mucins that are present in the gastrointestinal tract are MUC1, MUC2, MUC3A, MUC3B, MUC4, MUC5AC, MUC5B, MUC6, MUC12, MUC13, and MUC17 (Elzinga et al. 2021). The gel-

forming mucins the goblet cells express are MUC2, MUC5AC, MUC5B, and MUC6, from which MUC2 is the major mucin in the small intestine, and the others are mainly expressed in the stomach (Leteurtre et al. 2004). Earlier studies indicate that the MTX-differentiated HT-29 cells express MUC1, MU2, MUC3, and MUC5AC from which MUC5AC is the major mucin and MUC2 is secreted in low amounts (Huet et al. 1995, Gagnon et al. 2013, Martínez-Maqueda et al. 2015, Elzinga et al. 2021). Therefore, the DIF HT-29 cells in this study could be tested in the future with other MUC antibodies and analysed whether the cells express some of the other mucins, thus further verifying the differentiation and production of mucus. Especially the MUC5AC should be tested due to the abundance of this mucin in the HT-29 cells (Elzinga et al. 2021).

4.3 Successful infection with enteroviruses enables future research

Enteroviruses primarily infect through the faecal-oral route (Zhu et al. 2021). CVA9 has been studied at JYU in A549 lung cancer cells, but there is an interest for studying the virus in the HT-29 intestinal cell type as well. Therefore, the DIF and unDIF HT-29 cells were infected with CVA9 to test the capability of infection by the virus. The infection capability of CVA9 in the HT-29 cells (Figure 8) was somewhat expected, as these cells are similar with the epithelial cells of small intestine, which is part of the faecal-oral route. The receptors CVA9 is believed to use for entering the cells are αV integrins, glucose-regulated protein 78 A, subunit of major histocompatibility complex class I (MHC-I) antigen, and 2-microglobulin (Huttunen et al. 2014). From the αV integrins, αVβ6 seems to be a high-affinity receptor for the virus (Heikkilä et al. 2009). The HT-29 cells express the RGD-binding integrin αV that associates with β6 (Rajan et al. 2018), hence, the virus can enter these cells and infect them.

CVB3 has also been studied at JYU in A549 cells, and similarly to CVA9, there is an interest to see if the HT-29 cells could be utilised with this virus, as well. Therefore, the DIF and unDIF cells were infected with CVB3 to test the viral infectivity of these cells. Similarly, to CVA9, CVB3 also infected the HT-29 cells (Figure 9). The receptors the CVB3 is believed to use to enter cells are coxsackievirus-adenovirus receptor (CAR) and decay-accelerating factor (DAF) (Fu and Xiong 2023). Because the virus was able to infect these cells, it indicates that HT-29 cells express one or both of these receptors.

OC43 coronavirus has been studied at JYU, as well, but in MRC-5 lung fibroblasts. Primarily the OC43 virus causes upper respiratory tract disease (Liu et al. 2021), yet, the virus can also cause gastrointestinal symptoms (Luo et al. 2020). Hence, there was an interest to evaluate whether OC43 could infect the HT-29 cells as well, and if these cells could then be used in studying this virus. Therefore, the DIF and unDIF HT-29 cells were infected with OC43 for five days. Despite the three replicate analyses and various tested infection doses, infection did not occur (Figure 10). This is explainable by looking at the receptors the virus

uses for cell entry. The receptors OC43 uses are the glycan-based receptors carrying 9-O-acetylated sialic acid (Szczepanski et al. 2019). Because the virus was not able to infect these cells, it indicates that the needed receptor for OC43 virus is not found in HT-29 cells.

The verification of CVA9 and CVB3 infectivity in these cells was important for the future usability of the HT-29 cell line in investigations of CVA9 and CVB3 behaviour in cells. The HT-29 cells closely resemble the conditions in the primary infection site of these viruses, which gives better understanding of their viral life cycle. The whole life cycle with its essential steps, like cell entry and replication, can be uncovered by investigating the viruses in cell models that closely resemble their target infection site in humans. For example, the previous studies of viral life cycle in cell models, like the study of Huttunen and colleagues (2014), have revealed the receptors that the viruses use for cell entry.

Precise knowledge of the life cycle of the viruses is also crucial in the attempts to develop antivirals, vaccines, and other treatment against them. One exemplary example of this is the successful development of human immunodeficiency virus (HIV) medication which is one of the major accomplishments in biomedicine (Fauci et al. 2013). Exact knowledge about the phases of HIV life cycle enabled the development of anti-HIV drugs that could be targeted to inhibit certain points of infection (Mehellou and De Clercq 2010). An example of enteroviruses is the poliovirus vaccine, which was developed after studying the virus also in cell models (Baicus 2012). As there are currently no vaccines or medication available for non-polio enteroviruses, like CVA9 and CVB3 (Ho et al. 2016), extensive research is needed in the future, for which cell models are a vital tool. There are studies of antivirals against enterovirus 71 causing hand, foot, and mouth disease (Zhu et al. 2011) and enterovirus D68 that can cause acute flaccid myelitis (Hu et al. 2020), but those are still at their infancy.

4.4 *P. aeruginosa* infectivity enhances possibility for future studies

The DIF and unDIF HT-29 cells were infected with *P. aeruginosa* strains PA14 and 573, *S. typhimurium*, *Str. mutans,* and *A. baumannii* to test which bacteria could be investigated with this cell model. The infectivity of both *P. aeruginosa* strains in these cells was somewhat expected as these bacteria can infect multiple cell types of humans through ingestion of *P. aeruginosa* -contaminated water (Loveday et al. 2014). Furthermore, the PA14 strain is known to be hypervirulent (He et al. 2004), so its infectivity was anticipated, and it was therefore, used as the primary bacterium in the infection tests. Due to its hypervirulence, PA14 probably infected the cells already within 5.5 h (Figure 7) while the strain 573 needed 3 d (Figure 12B). The mucus did not protect the DIF HT-29 cells from infection as there was no significant difference in the infectivity of DIF and unDIF cells.

In the 3 d infection test, the significance of infection could not be determined due to the biofilm formation (Figure 11A) that occurred in both strains. As biofilm

formation is a notable resistance factor of *P. aeruginosa* (Ciofu and Tolker-Nielsen 2019), this cell mode could be used in future studies focusing on investigating the course of biofilm formation in these strains. Questions like when does the biofilm formation start, could be investigated further. In this study the biofilms were not formed in the 1 d infection but were clearly visible in the 3 d infection and therefore, future studies could determine the actual time of biofilm formation. This knowledge would truly be important and relevant because *P. aeruginosa* forms biofilms in humans on for example urinary catheters and implant devices like artificial joints, causing severe nosocomial infections and chronic infections (Cole et al. 2014, Cerioli et al. 2020). Precise knowledge of the course of biofilm formation could help in developing treatments that would prevent biofilm formation and thus expose the bacteria better to antibiotics. The absence of biofilms could aid the investigations further in understanding the other resistance mechanisms of biofilm than only being a physical barrier, as some antibiotics can penetrate the biofilm but are still unable to kill the bacterium inside it (Mulcahy et al. 2014).

In addition, future studies about the course of *P. aeruginosa* infection could reveal how and when the bacterium secretes its numerous virulence factors (Cepas and Soto 2020) and how the secretion affects the cells. HT-29 cells have been used in studies of toxin ExoS (Fraylick et al. 2001, Rocha et al. 2005) and exopolysaccharides (Tahmourespour et al. 2020) that *P. aeruginosa* secretes with results of changes in cell morphology. However, these studies have used the unDIF HT-29 cells and therefore knowledge about the effect of DIF cell's mucus against the bacterium and its toxins remains to be investigated.

4.5 Unexpectedly mild *S. typhimurium* infection

The mildness of *S. typhimurium* infection was a bit surprising (Figure 13A). *S. typhimurium* is an intestinal bacterium transmitted through faecal-oral route (Gal-Mor et al. 2014) so it was thought to be highly infective towards the HT-29 cells. Furthermore, the HT-29 cells along with another intestinal colon adenocarcinoma cell line Caco-2 have been used in earlier studies of *S. typhimurium*, hence the expectation of infectivity (Kim et al. 1998, Kortman et al. 2012, Gagnon et al. 2013, Dostal et al. 2014, Ostovan et al. 2021, Fonseca et al. 2021). Interestingly, the *S. typhimurium* infection was ~10% stronger in the unDIF cells (Figure 13A). This finding contradicts with an earlier study of Gagnon and colleagues (2013) where they infected unDIF and mucus-producing MTX-differentiated HT-29 cells with different *S. typhimurium* strains and discovered, that the bacteria adhered to and invaded the mucus-producing cells more than the unDIF HT-29 cells. The opposite results of this study could indicate that the strain used here behaves differently than the strains used in the study of Gagnon and colleagues (2013). Additionally, two different methods were used in this study and the study of Gagnon and colleagues to differentiate the HT-29 cells, and therefore, the

percentage of mucus-producing cells could differ in the used cell models, hence, the results in *S. typhimurium* adhesion and invasion vary.

However, future studies should focus on the hypothesis, that the mucus produced by the DIF HT-29 cells protected the DIF cells from a stronger infection by the *S. typhimurium* strain used here. For example, Zarepour and colleagues (2013) discovered in their study using mice, that the intestinal mucus and MUC2 mucin, both investigated also in this study, limited the ability of *S. typhimurium* to colonise and to interact with the intestinal epithelium, also reducing mortality of the mice. If this could be verified with the HT-29 cell model of this study, it would give new insights about the role of mucus in the human small intestine. Furthermore, a longer infection time should be investigated to assess, whether the mild infection seen here was only an early phase of the infection. A longer infection time could amplify the difference in the strength of the infection between the DIF and unDIF HT-29 cells, thus verifying the hypothesis that mucus protected the DIF cells from *S. typhimurium* infection.

Overall, novel research of *S. typhimurium* is needed. The bacterium is one of the leading serotypes causing non-typhoid *Salmonella* infections worldwide, with >90 million cases of infection and >150 000 deaths annually (Mandal et al. 2021). Furthermore, multi-drug-resistant strains are emerging, leading to the need of discovering novel antibiotics (Eng et al. 2015). Cell models, like the HT-29 cell model established here, provide a good research tool for these studies. A considerable amount of *S. typhimurium* studies have been performed in murine models, revealing crucial knowledge about this bacterium (Barthel et al. 2003, Stecher et al. 2005, 2007, Moreira et al. 2010, Monack 2012, Zarepour et al. 2013), yet, these findings can't be directly applied to humans without additional studies due to the differences between the two species and the difference of the disease *S. typhimurium* causes in them. In humans the bacterium causes enterocolitis, while in mice it causes typhoid fever-like symptoms with intestinal lesions (Zhang et al. 2003). Thus, the HT-29 cell model would provide an important tool for examining the course of infection and host-pathogen interaction of the bacterium in humans and confirming whether the findings in murine models are applicable to humans. Furthermore, the discoveries of the studies using the HT-29 cell model could be utilised vice versa, applying the findings to murine models in which for example novel drugs can be investigated.

4.6 Possibility of mucosal protection against *Str. mutans* infection

The primary infection site for *Str. mutans* is the oral cavity (Metwalli et al. 2013) and therefore it is understandable that the infection in the HT-29 cells did not occur. However, similarly to *S. typhimurium*, there is a possibility that the mucus protected the DIF HT-29 cells from the infection as only the unDIF cells were mildly infected (Figure 13B). On the other hand, the mild infection detected here could be only the starting phase of the infection. Future studies should be

executed to reveal whether the mucus of DIF HT-29 cells has a protective role against the bacterium. Furthermore, a longer infection time should be included to see whether the bacterium needs even a longer time for the infection to occur. *Str. mutans* can also reside in the intestines (Forssten et al. 2010) so possibly the longer infection time on the HT-29 cells could cause an infection.

Overall, finding a suitable *in vitro* human cell model for *Str. mutans* is challenging because mimicking the conditions of teeth and oral cavity is difficult (Forssten et al. 2010). Berlutti and colleagues (2010) have used human gingival fibroblast cells, but mostly the bacterium has been studied in animal models, like rats and mice, and animal cell lines (Forssten et al. 2010, Pan et al. 2015, Nomura et al. 2020, Tonguc Altin et al. 2021, Wolfoviz-Zilberman et al. 2021). The finding here that *Str. mutans* infected the unDIF HT-29 cells mildly is a highly important discovery and could enable future studies with a novel cell model. The possibility of studying *Str. mutans* with this cell model would be of importance in the future to learn more about the role of the biofilms the bacterium produces and the phases of the infection the bacterium causes.

4.7 *A. baumannii* infectivity might be strain dependent

On the contrary to *Str. mutans*, the result that *A. baumannii* was not able to infect the cells was unexpected (Figure 13C). *A. baumannii* usually targets mucosal membranes and colonises epithelial cells (Harding et al. 2018), and therefore it was expected that the HT-29 cells would be infected. Furthermore, as the bacterium did not grow on the agar plates, that were cultured from the bacterial infection samples taken after the 3 d infection on 96-well plate before CPE analysis, the bacterium clearly was not alive after the infection period anymore. This discovery is quite contradictory, when considering the characteristics of *A. baumannii*. The bacterium is able to tolerate even harsh environmental stresses like desiccation (Isler et al. 2018), yet it could not remain viable in surroundings with nutrients from the cell culture medium and temperature of +37 °C mimicking the temperature of the human body. *A. baumannii* is an extra-cellular pathogen, though it has a zipper-like mechanism enabling its invasion into epithelial cells (Harding et al. 2018), which it possibly could have used if needed for survival. Studying the phases of the 3 d infection, that was studied here, in HT-29 cells with for example samples imaged with transmission electron microscope, could reveal the host-pathogen interaction that occurred between the cells and *A. baumannii*.

Possibly some other *A. baumannii* strain could be infective in these cells, for example, Tayabali and colleagues (2012) used *A. baumannii* Bouvet and Grimont (ATCC #9955) strain and successfully infected the unDIF HT-29 cells. Research with the AC-54 strain used here could be done with another cell model in the future. A549 cell model has been successfully used (Smani et al. 2011, Gaddy et al. 2012, Lázaro-Díez et al. 2016), as well as, human bronchial epithelial cell lines NCI-H292 (Lee et al. 2006, Choi et al. 2008) in the studies of *A. baumannii*

infectivity and behaviour. Therefore, the HT-29 cell model could possibly be used with another *A. baumannii* strain, or the strain used here could be studied in another cell model. Overall, intensive research of *A. baumannii* is needed because the bacterium causes severe nosocomial infections and has developed resistance towards a vast spectrum of antibiotics, especially colistin, making it almost impossible to treat (Kempf and Rolain 2012).

5 CONCLUSIONS

This study aimed to validate the HT-29 cell differentiation protocol and its use as a cell model with the studied pathogens. The differentiation protocol to mucus-producing HT-29 cells was successfully established as the Alcian blue dye stained the mucus the cells produced, while the unDIF cells remained unstained. However, more antibody tests could still be done, because the antibodies tested in this study did not further verify the success of differentiation. Enteroviruses CVA9 and CVB3 infected the cells along with *P. aeruginosa* bacteria strains PA14 and 573, and therefore the studied cells can be utilised as an infection model for these pathogens. Furthermore, the mild infections that occurred with *S. typhimurium* and *Str. mutans* indicate a possibility of using the HT-29 cells as an infection model with these bacteria as well, however, future studies are required to verify this discovery. Overall, the use of the established HT-29 cell model in studies of the analysed pathogens is important to learn more about the host-pathogen interactions of these pathogens. Furthermore, the future studies with this cell model enable the development of novel drugs and vaccines against these pathogens.

ACKNOWLEDGEMENTS

I would like to thank my supervisors Professor Lotta-Riina Sundberg and postdoctoral researcher Kati Karvonen for excellent guidance, support and help with the laboratory work and during the writing process. I would also like to thank Professor Varpu Marjomäki as a bonus supervisor. Special thanks to Marjomäki and Sundberg research groups for collegiate support and taking me as a part of the group. Additional thanks to postdoctoral researcher Mira Laajala for helping with mathematics and postdoctoral researcher Visa Ruokolainen for helping with the microscopes.

Jyväskylä May 31, 2023
Jenni Auramo

REFERENCES

Andino A. & Hanning I. 2015. *Salmonella enterica* : Survival, Colonization, and Virulence Differences among Serovars. *Sci. World J.* 2015: 1–16.

Antunes F., Andrade F., Araújo F., Ferreira D. & Sarmento B. 2013. Establishment of a triple co-culture in vitro cell models to study intestinal absorption of peptide drugs. *Eur. J. Pharm. Biopharm.* 83: 427–435.

Antunes L.C.S., Visca P. & Towner K.J. 2014. Acinetobacter baumannii: evolution of a global pathogen. *Pathog. Dis.* 71: 292–301.

Ashida H., Mimuro H., Ogawa M., Kobayashi T., Sanada T., Kim M. & Sasakawa C. 2011. Cell death and infection: A double-edged sword for host and pathogen survival. *J. Cell Biol.* 195: 931–942.

Baicus A. 2012. History of polio vaccination. *World J. Virol.* 1: 108–114.

Baker J.L., Faustoferri R.C. & Quivey R.G. 2017. Acid-adaptive mechanisms of Streptococcus mutans-the more we know, the more we don't. *Mol. Oral Microbiol.* 32: 107–117.

Barron S.L., Saez J. & Owens R.M. 2021. In Vitro Models for Studying Respiratory Host–Pathogen Interactions. *Adv. Biol.* 5: 2000624, doi: 10.1002/adbi.202000624.

Barthel M., Hapfelmeier S., Quintanilla-Martínez L., Kremer M., Rohde M., Hogardt M., Pfeffer K., Rüssmann H. & Hardt W.-D. 2003. Pretreatment of Mice with Streptomycin Provides a Salmonella enterica Serovar Typhimurium Colitis Model That Allows Analysis of Both Pathogen and Host. *Infect. Immun.* 71: 2839–2858.

Berlutti F., Catizone A., Ricci G., Frioni A., Natalizi T., Valenti P. & Polimeni A. 2010. Streptococcus mutans and Streptococcus sobrinus are able to adhere and invade human gingival fibroblast cell line. *Int. J. Immunopathol. Pharmacol.* 23: 1253–1260.

Birchenough G.M.H., Johansson M.E., Gustafsson J.K., Bergström J.H. & Hansson G.C. 2015. New developments in goblet cell mucus secretion and function. *Mucosal Immunol.* 8: 712–719.

Botelho J., Grosso F. & Peixe L. 2019. Antibiotic resistance in Pseudomonas aeruginosa - Mechanisms, epidemiology and evolution. *Drug Resist. Updat. Rev. Comment. Antimicrob. Anticancer Chemother.* 44: 100640, doi: 10.1016/j.drup.2019.07.002.

Brown S.P., Cornforth D.M. & Mideo N. 2012. Evolution of virulence in opportunistic pathogens: generalism, plasticity, and control. *Trends Microbiol.* 20: 336–342.

Centonze M., Berenschot E.J.W., Serrati S., Susarrey-Arce A. & Krol S. 2022. The Fast Track for Intestinal Tumor Cell Differentiation and In Vitro Intestinal Models by Inorganic Topographic Surfaces. *Pharmaceutics* 14: 218, doi: 10.3390/pharmaceutics14010218.

Cepas V. & Soto S.M. 2020. Relationship between Virulence and Resistance among Gram-Negative Bacteria. *Antibiotics* 9: 719, doi: 10.3390/antibiotics9100719.

Cerioli M., Batailler C., Conrad A., Roux S., Perpoint T., Becker A., Triffault-Fillit C., Lustig S., Fessy M.-H., Laurent F., Valour F., Chidiac C. & Ferry T. 2020. Pseudomonas aeruginosa Implant-Associated Bone and Joint Infections: Experience in a Regional Reference Center in France. *Front. Med.* 7, doi: 10.3389/fmed.2020.513242.

Cerqueira G.M. & Peleg A.Y. 2011. Insights into Acinetobacter baumannii pathogenicity. *IUBMB Life* 63: 1055–1060.

Chen B.-S., Lee H.-C., Lee K.-M., Gong Y.-N. & Shih S.-R. 2020. Enterovirus and Encephalitis. *Front. Microbiol.* 11, doi: 10.3389/fmicb.2020.00261.

Choi C.H., Lee J.S., Lee Y.C., Park T.I. & Lee J.C. 2008. Acinetobacter baumannii invades epithelial cells and outer membrane protein A mediates interactions with epithelial cells. *BMC Microbiol.* 8: 216, doi: 10.1186/1471-2180-8-216.

Chuang Y.-C., Sheng W.-H., Li S.-Y., Lin Y.-C., Wang J.-T., Chen Y.-C. & Chang S.-C. 2011. Influence of genospecies of Acinetobacter baumannii complex on clinical outcomes of patients with acinetobacter bacteremia. *Clin. Infect. Dis. Off. Publ. Infect. Dis. Soc. Am.* 52: 352–360.

Ciofu O. & Tolker-Nielsen T. 2019. Tolerance and Resistance of Pseudomonas aeruginosa Biofilms to Antimicrobial Agents-How P. aeruginosa Can Escape Antibiotics. *Front. Microbiol.* 10: 913, doi: 10.3389/fmicb.2019.00913.

Cole S.J., Records A.R., Orr M.W., Linden S.B. & Lee V.T. 2014. Catheter-Associated Urinary Tract Infection by Pseudomonas aeruginosa Is Mediated by Exopolysaccharide-Independent Biofilms. *Infect. Immun.* 82: 2048–2058.

Crabbé A., Ledesma M.A. & Nickerson C.A. 2014. Mimicking the host and its microenvironment in vitro for studying mucosal infections by Pseudomonas aeruginosa. *Pathog. Dis.* 71: 1–19.

Dong W., Matsuno Y. & Kameyama A. 2012. A procedure for Alcian blue staining of mucins on polyvinylidene difluoride membranes. *Anal. Chem.* 84: 8461–8466.

Dostal A., Gagnon M., Chassard C., Zimmermann M.B., O'Mahony L. & Lacroix C. 2014. Salmonella adhesion, invasion and cellular immune responses are differentially affected by iron concentrations in a combined in vitro gut fermentation-cell model. *PloS One* 9: e93549, doi: 10.1371/journal.pone.0093549.

Eckmann L., Kagnoff M.F. & Fierer J. 1993. Epithelial cells secrete the chemokine interleukin-8 in response to bacterial entry. *Infect. Immun.* 61: 4569–4574.

Elzinga J., Lugt B. van der, Belzer C. & Steegenga W.T. 2021. Characterization of increased mucus production of HT29-MTX-E12 cells grown under Semi-Wet interface with Mechanical Stimulation. *PLOS ONE* 16: e0261191, doi: 10.1371/journal.pone.0261191.

Eng S.-K., Pusparajah P., Ab Mutalib N.-S., Ser H.-L., Chan K.-G. & Lee L.-H. 2015. *Salmonella*: A review on pathogenesis, epidemiology and antibiotic resistance. *Front. Life Sci.* 8: 284–293.

Fauci A.S., Folkers G.K. & Dieffenbach C.W. 2013. HIV-AIDS: much accomplished, much to do. *Nat. Immunol.* 14: 1104–1107.

Ferraretto A., Bottani M., De Luca P., Cornaghi L., Arnaboldi F., Maggioni M., Fiorilli A. & Donetti E. 2018. Morphofunctional properties of a differentiated Caco2/HT-29 co-culture as an *in vitro* model of human intestinal epithelium. *Biosci. Rep.* 38: BSR20171497, doi: 10.1042/BSR20171497.

Fonseca H.C., Sousa Melo D. de, Ramos C.L., Dias D.R. & Schwan R.F. 2021. Probiotic Properties of Lactobacilli and Their Ability to Inhibit the Adhesion of Enteropathogenic Bacteria to Caco-2 and HT-29 Cells. *Probiotics Antimicrob. Proteins* 13: 102–112.

Forssten S.D., Björklund M. & Ouwehand A.C. 2010. Streptococcus mutans, caries and simulation models. *Nutrients* 2: 290–298.

Fraylick J.E., La Rocque J.R., Vincent T.S. & Olson J.C. 2001. Independent and Coordinate Effects of ADP-Ribosyltransferase and GTPase-Activating Activities of Exoenzyme S on HT-29 Epithelial Cell Function. *Infect. Immun.* 69: 5318–5328.

Fu Y. & Xiong S. 2023. Exosomes mediate Coxsackievirus B3 transmission and expand the viral tropism. *PLOS Pathog.* 19: e1011090, doi: 10.1371/journal.ppat.1011090.

Gaddy J.A., Arivett B.A., McConnell M.J., López-Rojas R., Pachón J. & Actis L.A. 2012. Role of Acinetobactin-Mediated Iron Acquisition Functions in the Interaction of Acinetobacter baumannii Strain ATCC 19606T with Human Lung Epithelial Cells, Galleria mellonella Caterpillars, and Mice. *Infect. Immun.* 80: 1015–1024.

Gagnon M., Zihler Berner A., Chervet N., Chassard C. & Lacroix C. 2013. Comparison of the Caco-2, HT-29 and the mucus-secreting HT29-MTX intestinal cell models to investigate Salmonella adhesion and invasion. *J. Microbiol. Methods* 94: 274–279.

Gal-Mor O., Boyle E.C. & Grassl G.A. 2014. Same species, different diseases: how and why typhoidal and non-typhoidal Salmonella enterica serovars differ. *Front. Microbiol.* 5, doi: 10.3389/fmicb.2014.00391.

Geisler A., Hazini A., Heimann L., Kurreck J. & Fechner H. 2021. Coxsackievirus B3—Its Potential as an Oncolytic Virus. *Viruses* 13: 718, doi: 10.3390/v13050718.

Givirovskaia D., Givirovskiy G., Haapakoski M., Hokkanen S., Ruuskanen V., Salo S., Marjomäki V., Ahola J. & Repo E. 2022. Modification of face masks with zeolite imidazolate framework-8: A tool for hindering the spread of COVID-19 infection. *Microporous Mesoporous Mater.* 334: 111760, doi: 10.1016/j.micromeso.2022.111760.

Harding C.M., Hennon S.W. & Feldman M.F. 2018. Uncovering the mechanisms of Acinetobacter baumannii virulence. *Nat. Rev. Microbiol.* 16: 91–102.

He J., Baldini R.L., Déziel E., Saucier M., Zhang Q., Liberati N.T., Lee D., Urbach J., Goodman H.M. & Rahme L.G. 2004. The broad host range pathogen *Pseudomonas aeruginosa* strain PA14 carries two pathogenicity islands harboring plant and animal virulence genes. *Proc. Natl. Acad. Sci.* 101: 2530–2535.

Heikkilä O., Merilahti P., Hakanen M., Karelehto E., Alanko J., Sukki M., Kiljunen S. & Susi P. 2016. Integrins are not essential for entry of coxsackievirus A9 into SW480 human colon adenocarcinoma cells. *Virol. J.* 13: 171, doi: 10.1186/s12985-016-0619-y.

Heikkilä O., Susi P., Stanway G. & Hyypiä T. 2009. Integrin alphaVbeta6 is a high-affinity receptor for coxsackievirus A9. *J. Gen. Virol.* 90: 197–204.

Herath M., Hosie S., Bornstein J.C., Franks A.E. & Hill-Yardin E.L. 2020. The Role of the Gastrointestinal Mucus System in Intestinal Homeostasis: Implications for Neurological Disorders. *Front. Cell. Infect. Microbiol.* 10, doi: 10.3389/fcimb.2020.00248.

Hietanen E. & Susi P. 2020. Recombination Events and Conserved Nature of Receptor Binding Motifs in Coxsackievirus A9 Isolates. *Viruses* 12: 68, doi: 10.3390/v12010068.

Ho B.-C., Yang P.-C. & Yu S.-L. 2016. MicroRNA and Pathogenesis of Enterovirus Infection. *Viruses* 8: 11, doi: 10.3390/v8010011.

Howard A., O'Donoghue M., Feeney A. & Sleator R.D. 2012. Acinetobacter baumannii: An emerging opportunistic pathogen. *Virulence* 3: 243–250.

Hsu E. & Du Pasquier L. (eds.). 2015. *Pathogen-Host Interactions: Antigenic Variation v. Somatic Adaptations*. Springer International Publishing, Cham.

Hu Y., Musharrafieh R., Zheng M. & Wang J. 2020. Enterovirus D68 Antivirals: Past, Present, and Future. *ACS Infect. Dis.* 6: 1572–1586.

Huet G., Kim I., Bolos C. de, Lo-Guidice J.M., Moreau O., Hemon B., Richet C., Delannoy P., Real F.X. & Degand P. 1995. Characterization of mucins and proteoglycans synthesized by a mucin-secreting HT-29 cell subpopulation. *J. Cell Sci.* 108: 1275–1285.

Huttunen M., Waris M., Kajander R., Hyypiä T. & Marjomäki V. 2014. Coxsackievirus A9 Infects Cells via Nonacidic Multivesicular Bodies Simon A. (ed.). *J. Virol.* 88: 5138–5151.

Isler B., Doi Y., Bonomo R.A. & Paterson D.L. 2018. New Treatment Options against Carbapenem-Resistant Acinetobacter baumannii Infections. *Antimicrob. Agents Chemother.* 63: 10.1128/aac.01110-18, doi: 10.1128/AAC.01110-18.

Jean A., Quach C., Yung A. & Semret M. 2013. Severity and outcome associated with human coronavirus OC43 infections among children. *Pediatr. Infect. Dis. J.* 32: 325–329.

Karvonen K., Nykky J., Marjomäki V. & Gilbert L. 2021. Distinctive Evasion Mechanisms to Allow Persistence of Borrelia burgdorferi in Different Human Cell Lines. *Front. Microbiol.* 12, doi: 10.3389/fmicb.2021.711291.

Kempf M. & Rolain J.-M. 2012. Emergence of resistance to carbapenems in Acinetobacter baumannii in Europe: clinical impact and therapeutic options. *Int. J. Antimicrob. Agents* 39: 105–114.

Kim J.M., Eckmann L., Savidge T.C., Lowe D.C., Witthöft T. & Kagnoff M.F. 1998. Apoptosis of human intestinal epithelial cells after bacterial invasion. *J. Clin. Invest.* 102: 1815–1823.

Kim J., Hegde M. & Jayaraman A. 2010. Co-culture of epithelial cells and bacteria for investigating host–pathogen interactions. *Lab Chip* 10: 43–50.

Knoop K.A. & Newberry R.D. 2018. Goblet cells: multifaceted players in immunity at mucosal surfaces. *Mucosal Immunol.* 11: 1551–1557.

Kortman G.A.M., Boleij A., Swinkels D.W. & Tjalsma H. 2012. Iron Availability Increases the Pathogenic Potential of Salmonella Typhimurium and Other Enteric Pathogens at the Intestinal Epithelial Interface. *PLoS ONE* 7: e29968, doi: 10.1371/journal.pone.0029968.

Kröger C., Dillon S.C., Cameron A.D.S., Papenfort K., Sivasankaran S.K., Hokamp K., Chao Y., Sittka A., Hébrard M., Händler K., Colgan A., Leekitcharoenphon P., Langridge G.C., Lohan A.J., Loftus B., Lucchini S., Ussery D.W., Dorman C.J., Thomson N.R., Vogel J. & Hinton J.C.D. 2012. The transcriptional landscape and small RNAs of *Salmonella enterica* serovar Typhimurium. *Proc. Natl. Acad. Sci.* 109, doi: 10.1073/pnas.1201061109.

Lamas A., Miranda J.M., Regal P., Vázquez B., Franco C.M. & Cepeda A. 2018. A comprehensive review of non-enterica subspecies of Salmonella enterica. *Microbiol. Res.* 206: 60–73.

Laparra J.M. & Sanz Y. 2009. Comparison of in vitro models to study bacterial adhesion to the intestinal epithelium. *Lett. Appl. Microbiol.* 49: 695–701.

Lázaro-Díez M., Navascués-Lejarza T., Remuzgo-Martínez S., Navas J., Icardo J.M., Acosta F., Martínez-Martínez L. & Ramos-Vivas J. 2016. Acinetobacter baumannii and A. pittii clinical isolates lack adherence and cytotoxicity to lung epithelial cells in vitro. *Microbes Infect.* 18: 559–564.

Le Guennec L., Coureuil M., Nassif X. & Bourdoulous S. 2020. Strategies used by bacterial pathogens to cross the blood–brain barrier. *Cell. Microbiol.* 22: e13132, doi: 10.1111/cmi.13132.

Lee J.C., Koerten H., Broek P. van den, Beekhuizen H., Wolterbeek R., Barselaar M. van den, Reijden T. van der, Meer J. van der, Gevel J. van de & Dijkshoorn L. 2006. Adherence of Acinetobacter baumannii strains to human bronchial epithelial cells. *Res. Microbiol.* 157: 360–366.

Leland D.S. & Ginocchio C.C. 2007. Role of Cell Culture for Virus Detection in the Age of Technology. *Clin. Microbiol. Rev.* 20: 49–78.

Lemos J.A., Palmer S.R., Zeng L., Wen Z.T., Kajfasz J.K., Freires I.A., Abranches J. & Brady L.J. 2019. The Biology of Streptococcus mutans. *Microbiol. Spectr.* 7: 7.1.03, doi: 10.1128/microbiolspec.GPP3-0051-2018.

Lesuffleur T., Barbat A., Dussaulx E. & Zweibaum A. 1990. Growth Adaptation to Methotrexate of HT-29 Human Colon Carcinoma Cells Is Associated with Their Ability to Differentiate into Columnar Absorptive and Mucus-secreting Cells1. *Cancer Res.* 50: 6334–6343.

Leteurtre E., Gouyer V., Rousseau K., Moreau O., Barbat A., Swallow D., Huet G. & Lesuffleur T. 2004. Differential mucin expression in colon carcinoma HT-29 clones with variable resistance to 5-fluorouracil and methotrexate. *Biol. Cell* 96: 145–151.

Limage R., Tako E., Kolba N., Guo Z., García-Rodríguez A., Marques C.N.H. & Mahler G.J. 2020. TiO2 Nanoparticles and Commensal Bacteria Alter Mucus Layer Thickness and Composition in a Gastrointestinal Tract Model. *Small Weinh. Bergstr. Ger.* 16: e2000601, doi: 10.1002/smll.202000601.

Liu D.X., Liang J.Q. & Fung T.S. 2021. Human Coronavirus-229E, -OC43, -NL63, and -HKU1 (Coronaviridae). *Encycl. Virol.*: 428–440.

Lopez D., Vlamakis H. & Kolter R. 2010. Biofilms. *Cold Spring Harb. Perspect. Biol.* 2: a000398–a000398, doi: 10.1101/cshperspect.a000398.

Loveday H.P., Wilson J.A., Kerr K., Pitchers R., Walker J.T. & Browne J. 2014. Association between healthcare water systems and Pseudomonas aeruginosa infections: a rapid systematic review. *J. Hosp. Infect.* 86: 7–15.

Luo X., Zhou G.-Z., Zhang Y., Peng L.-H., Zou L.-P. & Yang Y.-S. 2020. Coronaviruses and gastrointestinal diseases. *Mil. Med. Res.* 7: 49, doi: 10.1186/s40779-020-00279-z.

Mandal R.K., Jiang T. & Kwon Y.M. 2021. Genetic Determinants in Salmonella enterica Serotype Typhimurium Required for Overcoming In Vitro Stressors in the Mimicking Host Environment. *Microbiol. Spectr.* 9: e00155-21, doi: 10.1128/Spectrum.00155-21.

Martínez-Maqueda D., Miralles B. & Recio I. 2015. HT29 Cell Line. In: Verhoeckx K., Cotter P., López-Expósito I., Kleiveland C., Lea T., Mackie A., Requena T., Swiatecka D. & Wichers H. (eds.), *The Impact of Food Bioactives on Health: in vitro and ex vivo models*, Springer International Publishing, Cham, pp. 113–124.

Massilamany C., Gangaplara A. & Reddy J. 2014. Intricacies of cardiac damage in coxsackievirus B3 infection: Implications for therapy. *Int. J. Cardiol.* 177: 330–339.

Matsumoto-Nakano M. 2018. Role of Streptococcus mutans surface proteins for biofilm formation. *Jpn. Dent. Sci. Rev.* 54: 22–29.

Mehellou Y. & De Clercq E. 2010. Twenty-Six Years of Anti-HIV Drug Discovery: Where Do We Stand and Where Do We Go? *J. Med. Chem.* 53: 521–538.

Merritt J. & Qi F. 2012. The mutacins of Streptococcus mutans: regulation and ecology. *Mol. Oral Microbiol.* 27: 57–69.

Metwalli K.H., Khan S.A., Krom B.P. & Jabra-Rizk M.A. 2013. Streptococcus mutans, Candida albicans, and the human mouth: a sticky situation. *PLoS Pathog.* 9: e1003616, doi: 10.1371/journal.ppat.1003616.

Mikkelsen H., McMullan R. & Filloux A. 2011. The Pseudomonas aeruginosa Reference Strain PA14 Displays Increased Virulence Due to a Mutation in ladS. *PLOS ONE* 6: e29113, doi: 10.1371/journal.pone.0029113.

Monack D.M. 2012. Salmonella persistence and transmission strategies. *Curr. Opin. Microbiol.* 15: 100–107.

Moreira C.G., Weinshenker D. & Sperandio V. 2010. QseC mediates Salmonella enterica serovar typhimurium virulence in vitro and in vivo. *Infect. Immun.* 78: 914–926.

Morris F.C., Dexter C., Kostoulias X., Uddin M.I. & Peleg A.Y. 2019. The Mechanisms of Disease Caused by Acinetobacter baumannii. *Front. Microbiol.* 10, doi: 10.3389/fmicb.2019.01601.

Muehlenbachs A., Bhatnagar J. & Zaki S.R. 2015. Tissue tropism, pathology and pathogenesis of enterovirus infection. *J. Pathol.* 235: 217–228.

Muir P. 2017. Enteroviruses. *Medicine (Baltimore)* 45: 794–797.

Mulcahy L.R., Isabella V.M. & Lewis K. 2014. Pseudomonas aeruginosa Biofilms in Disease. *Microb. Ecol.* 68: 1–12.

Nikonov O.S., Chernykh E.S., Garber M.B. & Nikonova E.Yu. 2017. Enteroviruses: Classification, diseases they cause, and approaches to development of antiviral drugs. *Biochem. Mosc.* 82: 1615–1631.

Nomura R., Matayoshi S., Otsugu M., Kitamura T., Teramoto N. & Nakano K. 2020. Contribution of Severe Dental Caries Induced by Streptococcus mutans to the Pathogenicity of Infective Endocarditis. *Infect. Immun.* 88: 10.1128/iai.00897-19, doi: 10.1128/IAI.00897-19.

Olson J.C., Fraylick J.E., McGuffie E.M., Dolan K.M., Yahr T.L., Frank D.W. & Vincent T.S. 1999. Interruption of multiple cellular processes in HT-29 epithelial cells by Pseudomonas aeruginosa exoenzyme S. *Infect. Immun.* 67: 2847–2854.

Ostovan R., Pourmontaseri M., Hosseinzadeh S. & Shekarforoush S.S. 2021. Interaction between the probiotic Bacillus subtilis and Salmonella Typhimurium in Caco-2 cell culture. *Iran. J. Microbiol.* 13: 91–97.

Pan W., Fan M., Wu H., Melander C. & Liu C. 2015. A new small molecule inhibits Streptococcus mutans biofilms in vitro and in vivo. *J. Appl. Microbiol.* 119: 1403–1411.

Park J.-H., Lee J.-M., Lee E.-J., Kim D.-J. & Hwang W.-B. 2018. Kynurenine promotes the goblet cell differentiation of HT-29 colon carcinoma cells by modulating Wnt, Notch and AhR signals. *Oncol. Rep.* 39: 1930–1938.

Parker D., Cohen T.S., Alhede M., Harfenist B.S., Martin F.J. & Prince A. 2012. Induction of Type I Interferon Signaling by Pseudomonas aeruginosa Is Diminished in Cystic Fibrosis Epithelial Cells. *Am. J. Respir. Cell Mol. Biol.* 46: 6–13.

Pelaseyed T., Bergström J.H., Gustafsson J.K., Ermund A., Birchenough G.M.H., Schütte A., Post S. van der, Svensson F., Rodríguez-Piñeiro A.M., Nyström E.E.L., Wising C., Johansson M.E.V. & Hansson G.C. 2014. The mucus and mucins of the goblet cells and enterocytes provide the first defense line of the gastrointestinal tract and interact with the immune system. *Immunol. Rev.* 260: 8–20.

Pinkert S., Klingel K., Lindig V., Dörner A., Zeichhardt H., Spiller O.B. & Fechner H. 2011. Virus-host coevolution in a persistently coxsackievirus B3-infected cardiomyocyte cell line. *J. Virol.* 85: 13409–13419.

Rajan A., Persson B.D., Frängsmyr L., Olofsson A., Sandblad L., Heino J., Takada Y., Mould A.P., Schnapp L.M., Gall J. & Arnberg N. 2018. Enteric Species F Human Adenoviruses use Laminin-Binding Integrins as Co-Receptors for Infection of Ht-29 Cells. *Sci. Rep.* 8: 10019, doi: 10.1038/s41598-018-28255-7.

Ramos J.-L., Goldberg J.B. & Filloux A. (eds.). 2015. *Pseudomonas: Volume 7: New Aspects of Pseudomonas Biology*. Springer Netherlands, Dordrecht.

Rocha C.L., Rucks E.A., Vincent D.M. & Olson J.C. 2005. Examination of the Coordinate Effects of Pseudomonas aeruginosa ExoS on Rac1. *Infect. Immun.* 73: 5458–5467.

Schirtzinger E.E., Kim Y. & Davis A.S. 2022. Improving human coronavirus OC43 (HCoV-OC43) research comparability in studies using HCoV-OC43 as a surrogate for SARS-CoV-2. *J. Virol. Methods* 299: 114317, doi: 10.1016/j.jviromet.2021.114317.

Schmidt F. & Völker U. 2011. Proteome analysis of host-pathogen interactions: Investigation of pathogen responses to the host cell environment. *Proteomics* 11: 3203–3211.

Sears C.L. 2000. Molecular Physiology and Pathophysiology of Tight Junctions V. Assault of the tight junction by enteric pathogens. *Am. J. Physiol.-Gastrointest. Liver Physiol.* 279: G1129–G1134.

Simon-Assmann P., Turck N., Sidhoum-Jenny M., Gradwohl G. & Kedinger M. 2007. In vitro models of intestinal epithelial cell differentiation. *Cell Biol. Toxicol.* 23: 241–256.

Singhal T. 2020. A Review of Coronavirus Disease-2019 (COVID-19). *Indian J. Pediatr.* 87: 281–286.

Smani Y., Domínguez-Herrera J. & Pachón J. 2011. Rifampin Protects Human Lung Epithelial Cells Against Cytotoxicity Induced by Clinical Multi and Pandrug-resistant Acinetobacter baumannii. *J. Infect. Dis.* 203: 1110–1119.

Southwood D. & Ranganathan S. 2019. Host-Pathogen Interactions. In: Ranganathan S., Gribskov M., Nakai K. & Schönbach C. (eds.), *Encyclopedia of Bioinformatics and Computational Biology*, Academic Press, Oxford, pp. 103–112.

Spector M.P. & Kenyon W.J. 2012. Resistance and survival strategies of Salmonella enterica to environmental stresses. *Food Res. Int.* 45: 455–481.

Stecher B., Macpherson A.J., Hapfelmeier S., Kremer M., Stallmach T. & Hardt W.-D. 2005. Comparison of Salmonellaenterica Serovar Typhimurium Colitis in Germfree Mice and Mice Pretreated with Streptomycin. *Infect. Immun.* 73: 3228–3241.

Stecher B., Robbiani R., Walker A.W., Westendorf A.M., Barthel M., Kremer M., Chaffron S., Macpherson A.J., Buer J., Parkhill J., Dougan G., Mering C. von & Hardt W.-D. 2007. Salmonella enterica serovar typhimurium exploits inflammation to compete with the intestinal microbiota. *PLoS Biol.* 5: 2177–2189.

Szczepanski A., Owczarek K., Bzowska M., Gula K., Drebot I., Ochman M., Maksym B., Rajfur Z., Mitchell J.A. & Pyrc K. 2019. Canine Respiratory

Coronavirus, Bovine Coronavirus, and Human Coronavirus OC43: Receptors and Attachment Factors. *Viruses* 11: 328, doi: 10.3390/v11040328.
Tahmourespour A., Ahmadi A. & Fesharaki M. 2020. The anti-tumor activity of exopolysaccharides from Pseudomonas strains against HT-29 colorectal cancer cell line. *Int. J. Biol. Macromol.* 149: 1072–1076.
Tayabali A.F., Nguyen K.C., Shwed P.S., Crosthwait J., Coleman G. & Seligy V.L. 2012. Comparison of the Virulence Potential of Acinetobacter Strains from Clinical and Environmental Sources. *PLOS ONE* 7: e37024, doi: 10.1371/journal.pone.0037024.
Tonguc Altin K., Topcuoglu N., Duman G., Unsal M., Celik A., Selvi Kuvvetli S., Kasikci E., Sahin F. & Kulekci G. 2021. Antibacterial effects of saliva substitutes containing lysozyme or lactoferrin against Streptococcus mutans. *Arch. Oral Biol.* 129: 105183, doi:10.1016/j.archoralbio.2021.105183.
Unden G., Thines E., Schuffler A. & Selzer P.M. 2016. *Host - Pathogen Interaction: Microbial Metabolism, Pathogenicity and Antiinfectives*. John Wiley & Sons, Incorporated, Weinheim, GERMANY.
Vestby L.K., Grønseth T., Simm R. & Nesse L.L. 2020. Bacterial Biofilm and its Role in the Pathogenesis of Disease. *Antibiotics* 9: 59, doi:10.3390/antibiotics9020059.
Wang S.-H., Wang K., Zhao K., Hua S.-C. & Du J. 2020. The Structure, Function, and Mechanisms of Action of Enterovirus Non-structural Protein 2C. *Front. Microbiol.* 11, doi: 10.3389/fmicb.2020.615965.
Wattiau P., Boland C. & Bertrand S. 2011. Methodologies for Salmonella enterica subsp. enterica subtyping: gold standards and alternatives. *Appl. Environ. Microbiol.* 77: 7877–7885.
Wolfoviz-Zilberman A., Kraitman R., Hazan R., Friedman M., Houri-Haddad Y. & Beyth N. 2021. Phage Targeting Streptococcus mutans In Vitro and In Vivo as a Caries-Preventive Modality. *Antibiotics* 10: 1015, doi:10.3390/antibiotics10081015.
Yu Q., Wang Z. & Yang Q. 2011. Ability of Lactobacillus to inhibit enteric pathogenic bacteria adhesion on Caco-2 cells. *World J. Microbiol. Biotechnol.* 27: 881–886.
Zarepour M., Bhullar K., Montero M., Ma C., Huang T., Velcich A., Xia L. & Vallance B.A. 2013. The Mucin Muc2 Limits Pathogen Burdens and Epithelial Barrier Dysfunction during Salmonella enterica Serovar Typhimurium Colitis. *Infect. Immun.* 81: 3672–3683.
Zhang S., Kingsley R.A., Santos R.L., Andrews-Polymenis H., Raffatellu M., Figueiredo J., Nunes J., Tsolis R.M., Adams L.G. & Bäumler A.J. 2003. Molecular Pathogenesis of *Salmonella enterica* Serotype Typhimurium-Induced Diarrhea. *Infect. Immun.* 71: 1–12.
Zhang S., Tuo J., Huang X., Zhu X., Zhang D., Zhou K., Yuan L., Luo H., Zheng B., Yuen K., Li M., Cao K. & Xu L. 2018. Epidemiology characteristics of human coronaviruses in patients with respiratory infection symptoms and phylogenetic analysis of HCoV-OC43 during 2010-2015 in Guangzhou. *PLOS ONE* 13: e0191789, doi: 10.1371/journal.pone.0191789.

Zhao H., Wang J., Chen J., Huang R., Zhang Y., Xiao J., Song Y., Ji T., Yang Q., Zhu S., Wang D., Lu H., Han Z., Zhang G., Li J. & Yan D. 2022. Molecular Epidemiology and Evolution of Coxsackievirus A9. *Viruses* 14: 822, doi:10.3390/v14040822.

Zhao M., Wang M., Zhang J., Ye J., Xu Y., Wang Z., Ye D., Liu J. & Wan J. 2020. Advances in the relationship between coronavirus infection and cardiovascular diseases. *Biomed. Pharmacother.* 127: 110230, doi: 10.1016/j.biopha.2020.110230.

Zhu P., Chen S., Zhang W., Duan G. & Jin Y. 2021. Essential Role of Non-Coding RNAs in Enterovirus Infection: From Basic Mechanisms to Clinical Prospects. *Int. J. Mol. Sci.* 22: 2904, doi: 10.3390/ijms22062904.

Zhu Q.-C., Wang Y., Liu Y.-P., Zhang R.-Q., Li X., Su W.-H., Long F., Luo X.-D. & Peng T. 2011. Inhibition of enterovirus 71 replication by chrysosplenetin and penduletin. *Eur. J. Pharm. Sci.* 44: 392–398.